Review

Modified sulfonated polyphenylsulfone proton exchange membrane with enhanced fuel cell performance: A review

Nor Azureen Mohamad Nor [a,d], Mohamad Azuwa Mohamed [a,b,c,*], Juhana Jaafar [d,*]

[a] Department of Chemical Sciences, Faculty of Science and Technology, Universiti Kebangsaan Malaysia, Bangi, Selangor 43600 UKM, Malaysia
[b] Polymer Research Centre, Faculty of Science and Technology, Universiti Kebangsaan Malaysia, Bangi, Selangor 43600 UKM, Malaysia
[c] Fuel Cell Institute, Universiti Kebangsaan Malaysia, Bangi, Selangor 43600 UKM, Malaysia
[d] Advanced Membrane Technology Research Centre, School of Chemical and Energy Engineering, Faculty of Engineering, Universiti Teknologi Malaysia, Johor Bahru, Johor 81310, Malaysia

A R T I C L E   I N F O

A B S T R A C T

The fuel cell application is an imperative energy conversion transformation with impressive potential for Malaysian future vitality. The relatively small market of fuel cell technology in Malaysia, causing considerable development in the domestic market, should be created to ensure a noteworthy contribution to Malaysia's energy industry. Currently, the research towards advanced polymer electrolyte membranes that can provide high proton conductivity and good durability is actively being studied. This article reviews the promising properties of polyphenylsulfone (PPSU) polymer materials as proton exchange membranes. This alternative polymer material would be best to replace the costly and counter the drawbacks of the perfluorinated membranes in fuel cell systems. Unfortunately, the interconnected hydrophilic channels of PPSU polymers are not well developed as the Nafion membrane. Thus, the PPSU was modified by a sulfonation reaction to confer their protonic conduction properties. In addition, the modification of the highly sulfonated PPSU by thermal crosslinking as a potential technique to improve the mechanical and chemical durability of the PPSU was discussed. Further, the effect of mixing various additives to develop the PPSU nanocomposite membrane on proton conductivity, physicochemical properties, mechanical properties and fuel cell performance are also discussed in this work.

Contents

* Corresponding authors at: Department of Chemical Sciences, Faculty of Science and Technology, Universiti Kebangsaan Malaysia, Bangi, Selangor 43600 UKM, Malaysia (M.A. Mohamed); Advanced Membrane Technology Research Centre, School of Chemical and Energy Engineering, Faculty of Engineering, Universiti Teknologi Malaysia, Johor Bahru, Johor 81310, Malaysia (J. Jaafar).
   E-mail addresses: mazuwa@ukm.edu.my (M.A. Mohamed), juhana@petroleum.utm.my (J. Jaafar).

Introduction

Demanding energy has become crucial to provide sufficient energy access for human well-being, poverty alleviation and economic development, which is an ongoing and pressing challenge for global growth. The world consumed about 154,000 terawatt-hours of primary energy in 2017, more than 27 times from 1800 (5650 terawatt-hours). Typically, higher energy consumers come from higher country average income [1]. Our world's current energy system is highly dependent on fossil fuels that produce carbon dioxide and other greenhouse gases that become the primary reason for global climate change [2]. Nowadays, the world has transitioned from an energy system dominated by fossil fuels to a low-carbon emission system. Renewable energy technologies, including fuel cells, bioenergy, hydropower, solar, wind, and geothermal energy, are options for replacing fossil fuels [3,4]. The global fuel cell market was valued at USD 4.1 billion in 2020 and is expected to grow massively at a compound annual growth rate of 23.3 % for the following 8 years [5]. Fuel cell technology has considerable potential for energy conversion devices towards the Malaysian future energy. The significant contribution of fuel cell technology towards Malaysia's energy by 2060 should be achieved by the rapid development of this technology in the domestic market [6]. Proton exchange membrane fuel cell (PEMFC) comprises advantages over other types of fuel cells which it is light, compact and operate at lower temperatures making it suitable for small
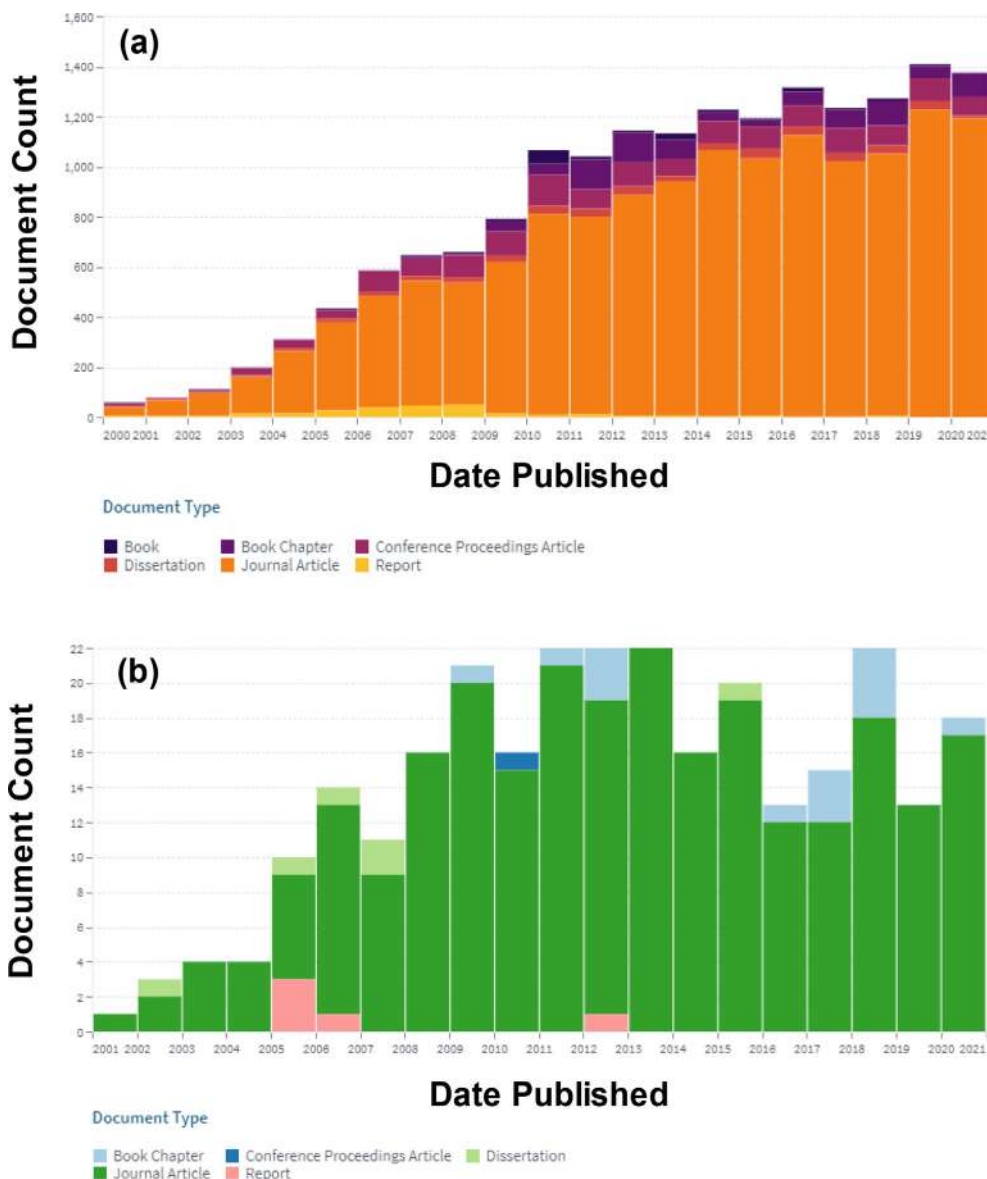

Fig. 1. The annual number of scholarly works on (a) PEM in fuel cell and (b) PPSU/PAES in fuel cell applications within year 2000 to 2021 (LENS. ORG scholar works search system, 2021).

operation devices like cars [7,8]. Development and operating cost are the primary factors that limit the commercialization of PEMFCs in the industry. Generally, the platinum catalyst of the electrodes and membrane electrolyte is a significant expensive contribution to PEMFC development [9]. Second is the storage problem for hydrogen gases which has a low density and combustible gas as a fuel that is necessary for installing the high-pressure hydrogen tank for mobile applications [10]. Water management in the fuel cell system becomes another hindrance in technology development where membrane materials research become challenging to make sure that it can effectively perform under different relative humidity and operating temperature conditions [11].

Currently, the research towards developing all fuel cell parts is actively being studied, especially the PEM. Based on the patent search system, the researchers reported that the PEM in fuel cell systems dramatically increased from 2000 to 2010 and steadily increased throughout the year until 2021 (See Fig. 1(**a**)). PEM is a semipermeable membrane that is designed as a medium for only proton transportation and, at the same time, blocking the fuel, reactant and electron from passing through the membrane [12]. The PEM performance is usually tested based on the proton conductivity, physicochemical properties, and membrane stability. Typically, proton conductivity values higher than 10^{-2} S cm^{-1} can be categorized as a good PEM, which can effectively transporting a proton [13]. They also require humidification to conduct protons, and sometimes due to hydration effects, the PEM will be degraded [14]. Other than that, an excellent dimensional, chemically, and thermally stable membrane under any operating conditions is another factor required as a PEM. The ability to be processed into a thin film and overall compatibility with other cell components is another property needed to develop an efficient cell performance [15]. PEM can be made from either pure polymer membranes or composite membranes. One of the most common commercially available PEM materials is a fluoropolymer (PFSA) and Nafion from DuPont. However, Nafion has a significant drawback in high operation temperature (>100 °C), leading to a relative decrease in the conductivity values. Meanwhile, Nafion membrane use at an operating temperature below 80 °C requires a fully saturated membrane, and it is too low for the cogeneration [16].

As a result, new proton conductor membranes that can withstand this condition are actively studied to develop flexible PEM resulting in excellent fuel cell performance. Recently, many research has been reported on a variety of new membrane materials for PEM development that has the potential to replace Nafion [17,18]. Among them are Polystyrene (PS)-based PEM [19,20], polyimide (PI)-based PEM [21,22], sulfonated polyphenylene-based PEM [23], polybenzimidazole (PBI)-based PEM [24,25], polysulfone (PSf)-based PEM [26], Polyether sulfone (PES)-based PEM [27], Polyphenylsulfone (PPSU)-based PEM [28,29], and natural polymer-based PEM [30] that have been reported as an alternative specialized PEM. Various types of alternative polymer-based PEM have been reported, and in this review, we are concentrating on describing the PPSU-based PEM for fuel cell applications. Polyphenylsulfone (PPSU) or also can be found as poly (arylene ether sulfone) (PAES) with a similar molecular structure, represents a sulfone polymer group that has been widely explored as an alternative to the proton-conducting membrane. The data obtained from the patent search system; the reviewed literature suggest that interest in PPSU as a proton exchange membrane has contributed to about two per cent of total publications of PEM in the fuel cell. The total number of documents found in the year 2000–2020 that deal specifically with PPSU/PAES membranes in fuel cell systems are presented in Fig. 1 (**b**). The excellent thermal stability and high mechanical strength of PPSU polymers make the PPSU one of the alternative materials to replace perfluorinated membranes as PEM [31]. Unfortunately, there is a restriction on

PPSU membrane to be applied in fuel cell applications as the proton conductivity of PPSU polymers is generally lower than perfluoro ionomers-based PEM membranes. The interconnected hydrophilic channels of PPSU polymers are not well developed as perfluoro-ionomers PEM [32]. Incorporating the inorganic materials into the polymer matrix becomes an efficient approach for improving the proton conductivity of the SPPSU membrane [33]. The incorporation of inorganic nanomaterials influences the organic phase's properties towards physicochemical properties, proton conductivity, and membrane stability that can result in excellent cell performance [34]. The intrinsic properties of the fillers, such as size, type, structure, and interactions with the polymer matrix, can significantly affect the resultant matrix [35,36].

The main objective of this review is to describe the vital aspect of PEMFC technology and the limitation of commonly available Nafion membrane operating under an extensive range of temperatures as a PEM. To the best of our knowledge, comprehensive reviews focusing on the in-depth understanding of modifications, physicochemical properties, and fuel cell performance of PPSU as a polymer backbone to develop the PEM are still limited. Compared to the other relevant reviews in the literature, this review focuses mainly on the chemical modifications and nanomaterials additions of PPSU to be comparable with the Nafion membrane in terms of physicochemical properties and fuel cell performance. A critical overview of the limitations of Nafions as PEM for the fuel cell application is addressed. This review also emphasized on the chemical modifications of PPSU through sulfonation reaction, thermal crosslinking as well as copolymer modifications to enhance the physicochemical properties and proton conductivity of the polymers has been discussed. The challenges of incorporating different types and structures of nanomaterials to build the sulfonated PPSU nanocomposite membrane and the improvements in its properties and fuel cell performance were also highlighted. The primary outcome of this study will benefit the scientific community in the sense of filling in the knowledge gap in multiple fields that encompass the PPSU nanocomposite membrane as PEM. Considering that the proton conductivity and durability of the SPPSU nanocomposite membrane are comparable to the commercial Nafion membrane, it could diversify its potential in fuel cell applications. The resourceful approach, which combines the unique properties of the polymers with different filler structures, is excellent potential to replace the commercial Nafion membrane in PEMFC applications.

Operating conditions of proton exchange membrane fuel cell

PEMFC is one of the alternative fuel cell types to replace the ageing alkaline fuel cell (AFC) technology that is mainly used in the space shuttle. This type of fuel cell is mainly being developed for transport, stationary and portable devices [37]. The simple structure of the PEMFC make it become the most fuel cell type studied by the researcher that can be applied in a wide range of applications, and many prototypes based on the PEMFC concepts are already available. This tremendous development of PEMFC has prepared a platform for an automaker to release fuel cell-powered hybrid vehicles into commercialization. The chemical reactions that produce the current are the key to how a fuel cell works (see Fig. 2). There are several kinds of fuel cells, and each operates differently according to the purpose of the technology. Like batteries, cathode and electrolyte are essential parts in PEMFC arrangements. The two electrodes, which are the positive (cathode) and negative (anode) site, is separated by an electrolyte layer which is determined as PEM in PEMFC systems [38]. The benefit of this technology as compared to the battery is that it can continuously generate electricity as long as fuel is supplied [39]. In this
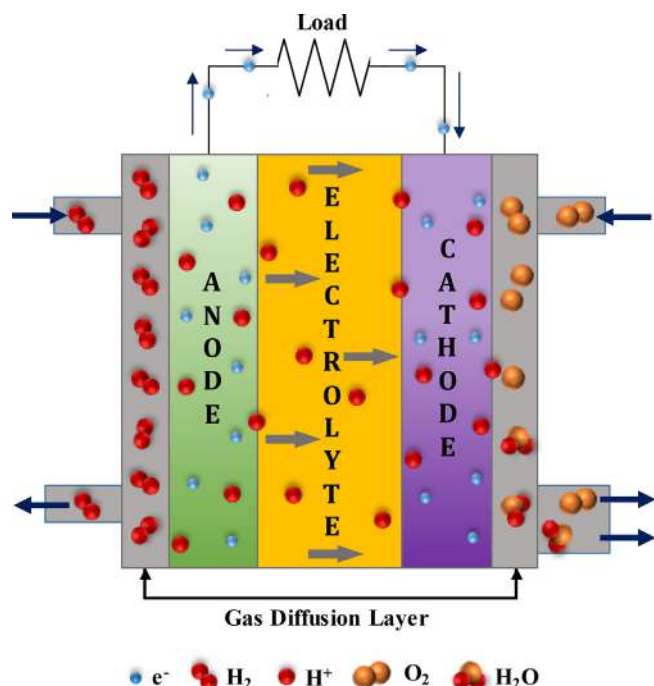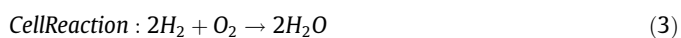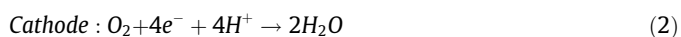
Fig. 2. The working concept in proton exchange membrane fuel cells.

case, hydrogen gas is used as a fuel, and it can be derived from various hydrocarbon sources, and only water and heat would be generated using pure hydrogen gases [40]. The electrochemical reaction that occurred in the PEM cell for power generation involves hydrogen as a fuel as follows:

$$Anode : 2H_2 \rightarrow 4H^+ + 4e^- \quad (1)$$

$$Cathode : O_2 + 4e^- + 4H^+ \rightarrow 2H_2O \quad (2)$$

$$CellReaction : 2H_2 + O_2 \rightarrow 2H_2O \quad (3)$$

Optimum operating conditions for a fuel cell are essential to obtain good fuel cell performance. The fuel cell performance was significantly affected by the operating conditions. The flow rate of the reactants (fuel and oxidants), operating pressure, temperature, and humidity of the fuel and oxidants are the parameters that affect the fuel cell performance. Ogungbemi *et al.* [41] highlighted the operating conditions, design parameters, and material properties of PEMFC in their review. Pressure is one of the significant parameters affecting the cell performance, in which performance will improve along increasing pressure. Unfortunately, high pressure requires gas compression and storage, while the pressurization of the fuel will affect the water management in the cell [42]. More than that, the gas pressure will also affect the operating of cell parameters such as inlet fuel composition, gas diffusion and flow-field plate design, which requires analysis of the fuel cell performance from a system perspective [43]. The reactant flow rate is another operating condition that will affect cell performance. The general requirement of the reactant flow is that it should be supplied equal to or greater than the reactants consumed within the cell, which should be appropriate for the required current [4244]. Other than the flow rate, the humidity conditions of the reactants gas should be achieved about 70 % to result in an excellent fuel cell performance [45]. The membrane dehydration and performance degradation happen when the electro-osmotic drag from the anode exceeds transport to the anode by back diffusion at high current density. Oxidants in low humidity conditions can worsen this

dehydration effect by reducing the back diffusion transportation from the cathode, which requires humidifying conditions at the anodes gasses [46].

There is an optimal temperature for each fuel design that led to explicitly choosing the optimum operating temperature for each fuel cell system. Controlling the operating temperature is crucial as the heat generated from electrochemical reactions will affect many factors, and it is very hard to maintain the optimum temperature. Increasing the operating temperature and pressure of the cell system causes more extensive ion mobility that enhances the ion conductivity [41]. As water is the main substance for humidity supply, the higher operating temperature will force the heat waste into the latent heat of vaporization results in more vaporized water, causing less water to be pushed out of the cell [47,48]. In contrast, low operating temperatures result in shorter warm-up times and also lowering the thermomechanical stresses. The upper limit of operating temperature depends on the electrolyte's properties used in the fuel cell system. Usually, the operating temperature for PEMFCs is restricted to approximately 90 °C because water evaporates from the polymer membrane, dries the membrane out, and causes the performance to drop quickly. PEMFC operating at a small temperature range (60 to 120 °C) restricted this system for broad applications. Therefore, there are increasing demands for a stable polymer membrane that can withstand the PEMFCs systems operating in wide range of temperatures.

PEMFC works under operating temperature of 80 °C, giving a system efficiency about 40–50 % and general output of about 50 W – 250 kW [49]. Solid and flexible membrane electrolyte as a heart of PEMFC system that operates at low enough temperature which will not leak, which remark as a superior alternative to replace the liquid electrolyte for AFC. However, the slow reduction reaction at the cathode in this cell required the platinum catalyst to fasten the reaction, simultaneously raising the operating cost [50]. Generally, the polymer electrolyte membrane has several required properties to be compatible with the fuel cell operation. PEM should be chemically stable as it acts in a strongly acidic medium and has high durability and fuel cell operation [51]. Ideally, the proton conductivity of the developed PEM that meets the PEMFC application requirement is about 0.1 S cm^{-1} [13]. Finally, all these properties should remain unchanged at the working temperature to avoid structural changes during the chemical reactions and be thermally stable [52]. The general PEM fuel cell flow arrangements as was depicted in Fig. 3. DuPont's Nafion-based polymer electrolyte membrane has excellent proton conductivity with high hydrolytic and oxidative stability, becoming the most commonly available PEM in the industry [53]. The state-of-the-art PEM fuel cells-based perfluorosulfonic acid ionomers such as Nafion, which shows good durability and high proton conductivity, is recognized as the most used PEM in the market [54].

State of the art and limitation of Nafion as proton exchange membrane

PEM is built in the fuel cell systems as a reactant separator and proton transportation medium, which was also functioning by blocking the electronic pathway through the membrane [12]. PEM can be made from either pure polymer membranes or composite membranes. One of the most common commercially available PEM materials is a fluoropolymer (PFSA) and Nafion from DuPont [16]. The PEM performance is usually tested based on the proton conductivity, physicochemical properties, and membrane stability. The general requirement for a good PEM has a higher proton conductivity ($>10^{-2}$ S cm^{-1}) that enables the proton transport between the electrodes [13]. They also require humidification to conduct protons, and sometimes due to hydration effects, the
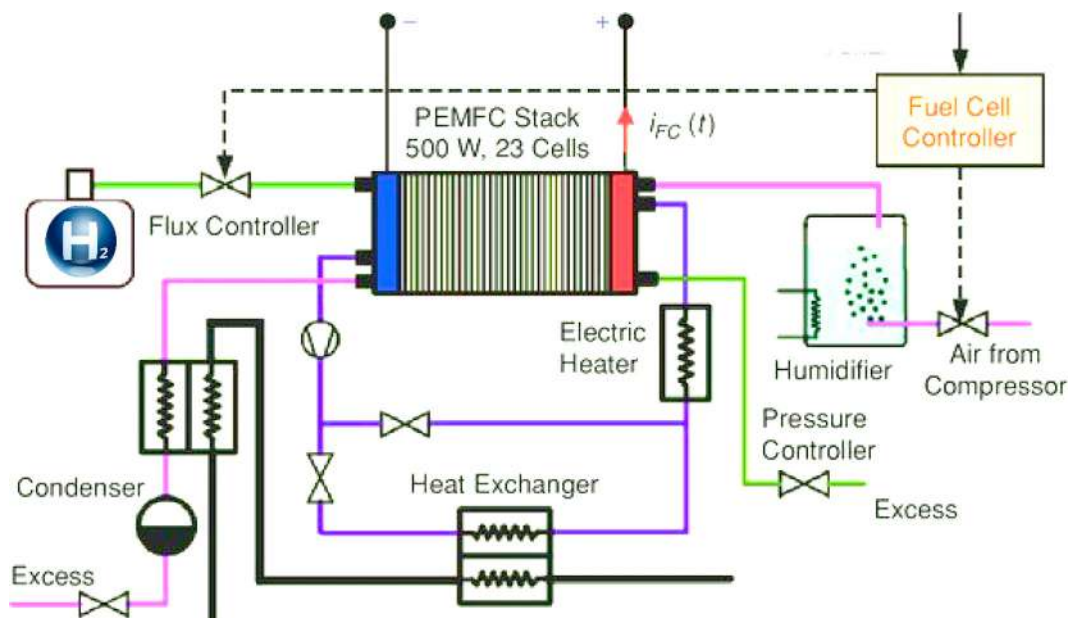
Fig. 3. Simplified diagram of the fuel cell flow system. Reprinted with permission from Ref. [55]. Copyright (2008) IEEE.

PEM will be degraded [14]. Exceptional dimensional, chemical, and thermal stability are the required properties for the PEM to operate under fuel cell operating conditions. The ability to be processed into a thin film and compatibility with other cell components is another property needed to develop efficient cell performance. The limitation of the PEM fuel cells-based perfluorosulfonic acid ionomers from commercialization is due to the expensive materials, low proton conductivity along temperature rising that contribute to water management issues and carbon monoxide poisoning [16]. PEM materials based on perfluorinated ionomer membranes such as the Nafion membrane are widely practiced and have become the general reference or benchmark for new membrane materials research. This membrane is a proton conductive polymer film that allows the only proton to cross over through the layer. Nafion is a brand name for a sulfonated tetrafluoroethylene-based fluoropolymer discovered by Walther Grot of DuPont in the late 1960 s. It has been broadly used for PEMFCs and can be identified based on various thicknesses and specific applications, which has been classified that Nafion 1110, Nafion 117, Nafion 115, Nafion 212, and Nafion 211 membranes are non-reinforced films [56]. The Nafion membrane-type's last number refers to several membrane thickness dimensions (Nafion 212–0.002 inches, Nafion 211–0.001 inches).

Different conditions in operating the fuel cell system required the different thicknesses of the Nafion membrane. A thicker membrane is needed when the fuel cell operates under high differential pressure and vice versa. The thicker Nafion membrane available in the market is Nafion 1110, with a membrane thickness of 254 μm. Nafion polymers' uniqueness resulted from incorporating perfluoro vinyl ether groups terminated with sulfonic acid groups onto a tetrafluoroethylene (PTFE) backbone [57]. Having high proton conductivity while maintaining excellent thermal and mechanical stability makes Nafion become considerable attention as PEM [58]. The chemical structure of Nafion is illustrated in Fig. 4(**a**). The morphology of Nafion membrane membranes is a matter of continuing study to allow for greater control of its properties. The Nafion structure will affect the important properties as PEM, such as water capacity, hydration stability at high temperatures and membrane durability [59]. The first Nafion model called the cluster channel or cluster-network model, consisted of an equal distribu-

tion of sulfonate ion clusters with a 40 Å (4 nm) diameter held with a continuous fluorocarbon lattice is illustrated in Fig. 4(b). The interconnection between the clusters in Nafion structures having narrow channels about 10 Å (1 nm) in diameter can explain the transport properties within the Nafion membrane [60]. The molecular structure, model cluster network, and proton transport of the Nafion membrane are shown in Fig. 4. This fluorinated polymer occasionally branches off into side chains with sulfonic acid groups. This sulfonic acid group forms the channels that allow proton transport from one side of the membrane to another [61]. The transportation models in the Nafion membrane are illustrated in Fig. 4 (**c**). Combining the stable PTFE backbone with the acidic sulfonic groups gives Nafion its excellent characteristics as proton conductive polymers. Nafion is widely been used as an electrolyte in a wide variety of applications such as vanadium redox flow batteries [62,63], fuel cell [53,64], water electrolyzers [65], and CO_2 separation [66]. Furthermore, the proton conductivity of the Nafion membrane can achieve up to 0.2 S cm^{-1} depending on the operating temperature and hydration state.

Although the Nafion membrane is the most commonly used fuel cell system, the high material and manufacturing cost due to the expensive Nafion materials and cathode platinum catalyst has restricted its function [68]. Nafion materials costing as much as about 100 times as compared to the engineering thermoplastic materials, which donating a big part in membrane manufacturing cost [69]. Furthermore, Nafion faces the problem of being highly dependent on the relative humidity of the cell, that results in reducing mechanical and dimensional stability at high operation temperature (>100 °C) [70]. Some studies have been reported on modifying Nafion by composite with another material to serve this PEM that can function in higher operating temperature [71,72]. The operating temperature below 80 °C is too low for cogeneration, and the PEM must be water-saturated. Fuel cell system without additional humidifiers is highly dependent on the rapid water generation through electrochemical reaction as well as the back diffusion through the membrane layer. That is become a turning point to explore high-temperature PEMFCs working between 100–200 °C as an alternative to cell system without additional humidifiers that can also potentially benefits electrode kinetics, proper heat management and excellent tolerance towards fuel impurities
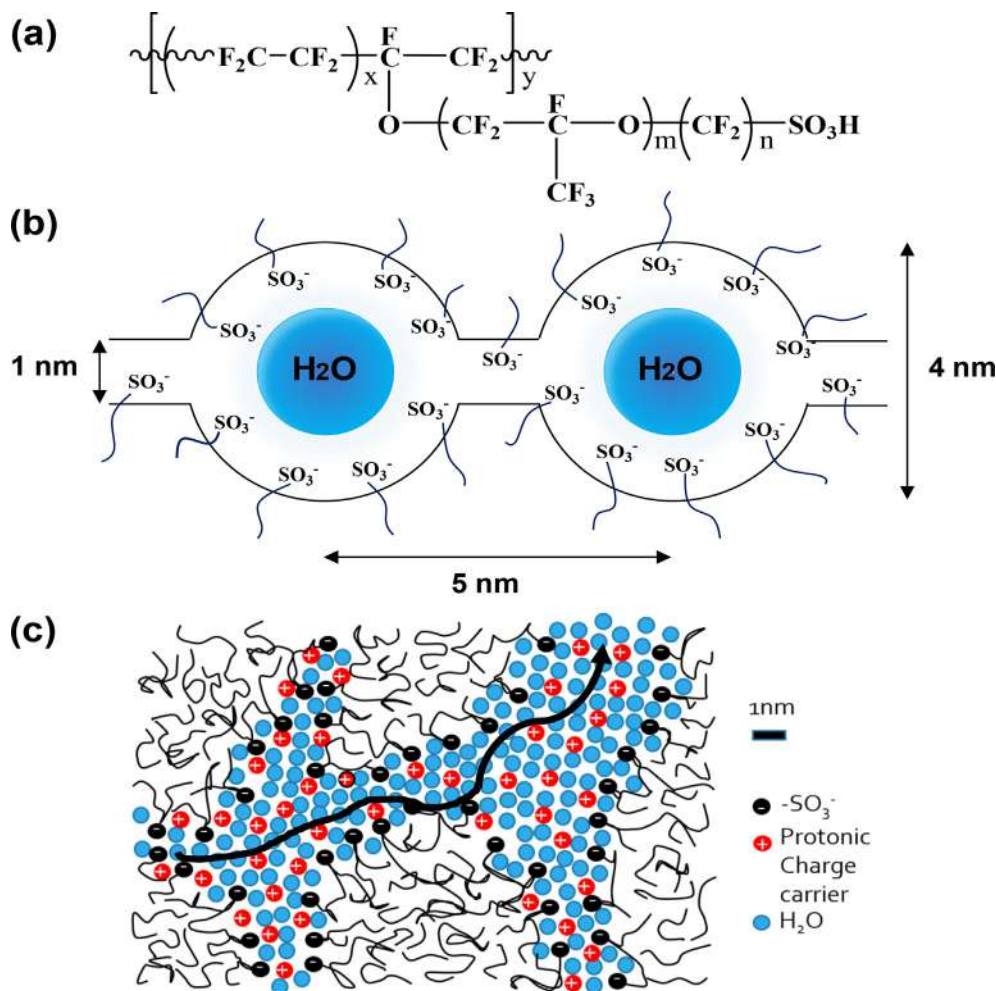
Fig. 4. (a) Nafion molecular structure, (b) model of cluster network. Reprinted (adapted) with permission from Ref. [15]. Copyright (2019) John Wiley and Sons, and (c) proton transport in Nafion. Reprinted (adapted) with permission from Ref. [67]. Copyright (2001) Elsevier.

that could lead to higher overall system efficiencies [60]. Unfortunately, these gains have yet to be realized as high cell temperature will cause the membrane loses its function rapidly, which contributes to shortening the membrane lifetime. This matter has to gain attention to research new anhydrous proton conductor membranes that can withstand under a broad range of cell operating conditions that will result in excellent cell performance and durability [17,25].

The polyphenylsulfone-based polymer as promising proton exchange membrane, and the chemical modifications

Generally, there are several required properties of the PEM to be compatible with the operation of various fuel cell types. PEM should be chemically stable as it acts in a strongly acidic medium [51]. Ideally, the durability and mechanical strength of the properties are desired in whatever the hydration state and the temperature of the membrane. The degradation phenomenon of the proton exchange membrane in the fuel cell system is thought to be caused by the H· or HO· or HO$_2$· radicals that occur at both electrodes. The degradation occurs at the anode by HO· or HO$_2$· radicals, which are thought to be formed by the reaction of H· radicals with O$_2$, which diffuses through the electrolyte from the cathode side. Meanwhile, another degradation at the cathode side

occurs from the HO· or HO$_2$· radicals originated during the cathode reduction reaction [73]. On the other hand, membrane degradation during single-cell operation is considered to result from the formation of HO· or HO$_2$· radicals [74]. Therefore, the chemical stability of the developed PEM materials in harsh oxidation conditions must be considered for PEM fabrication. In addition, water uptake is a crucial property for evaluating the efficiency of a PEM concerning proton conductivity. Water uptake by the membrane leads to dimensional changes that can adversely affect proton transportation across the membrane [75]. Besides, substantial changes in the dimensions would loosen the polymer matrix, creating large spaces between the polymer chains that lead to undesired cations that could pass through the electrolyte, contributing to performance deterioration.

Therefore, new proton conductor membrane materials have been extensively studied to produce a suitable PEM that can withstand a broad range of cell operating conditions that use non-fluorinated polymers [76]. Sulfone polymer, which is an aromatic compound that contains sulfonic functional groups attached to two carbon atoms, has been extensively studied. This material is being demanded by various industries due to its excellent mechanical properties and is highly stable in prolonged exposure to water and chemicals. It also can be handled and withstand a broad range of temperatures from −40 °C to 204 °C [77]. Sulfone polymers can

be classified as relatively cheap and abundant raw material sources in conjunction with easy manufacture, good mechanical properties, and environmental resistance. Sulfone polymer is amorphous thermoplastics comprised of aromatic units bridged with sulfone, isopropylidene, or other moieties [78]. Sulfone polymer can be classified into three categories which are polysulfone (PSU) [79], polyphenylsulfone (PPSU) [31], and polyethersulfone (PES) [27,80] with excellent properties that have been studied for fuel cell applications. The molecular structure of these sulfone polymers is illustrated in Fig. 5. The adequate sulfonation degree of PSU and PES polymers is challenging as the polymers are mechanically weak under harsh sulfonation reactions, and insufficient sulfonation will limit the overall proton conductivity. In contrast, highly sulfonation will lead to a polymer chain breakage [81]. The inadequate sulfonation degree and the chain-scission degradation during the sulfonation reaction process have restricted PSU and PES usage as PEM. Therefore, PPSU, with the highest resistance, long-term stability, and a broad range of chemical compatibility and ease of sulfonation modification, has directed this polymer to be further explored as PEM-based polymeric materials [82].

PPSU is a transparent and rigid high-temperature engineering thermoplastics. It consists of two segments: sulfone and ether, which are connected by ether linkages. PPSU is also sometimes referred to as poly (arylene ether sulfone) (PAES) or poly (arylene

sulfone) (PAS), which is known for its excellent hydrolytic stability, high impact strength, and good chemical resistance [77,83]. The tremendous heat-resistant properties of PPSU make it ideal to be applied in the medical, electrical, electronics and even aerospace industries. PPSU has widely been explored as a membrane material in various applications and is listed in Table 1. Darvishmanesh *et al.* [84] reported the PPSU membrane promising for filtration in mild organic solvents with excellent stability. However, due to the hydrophobic nature, low permeability and high fouling restricted the PPSU membrane from widely used in water applications. Unfortunately, there is a restriction on PPSU membrane to be applied in fuel cell application as the proton conductivity of PPSU polymers is generally lower than perfluoro ionomers-based PEM membranes [85]. The interconnected hydrophilic channels of PPSU polymers are not well developed as perfluoro-ionomers PEMs. Therefore, PPSU is modified by functioning with sulfonic acid groups through chemical modifications such as sulfonation and copolymer modifications playing important roles in improving the proton conductivity and physicochemical properties of the PPSU membrane to be potentially applied as PEM in the fuel cell [32]. Furthermore, thermal crosslinking is another modification that can improve the properties of the sulfonated PPSU, which are discussed in the next section.

Sulfonation of polyphenylsulfone

Sulfonation is a major industrial chemical process used to make various products. Sulfonated terms of PPSU polymers refer to the presence of sulfonic acid (SO_3H) groups on the aromatic rings, in which a hydrogen atom is connected to the aromatic ring of the ether ketone unit is replaced by SO_3H groups [107]. Feng *et al.* [108] reported on the rheology and phase inversion behaviour of PPSU for membrane formation. This study highlights the behaviour of PPSU in membrane forming and the effect of modification of PPSU by sulfonation. In this state, the purpose of sulfonation is to reduce the tendency of membrane fouling and enhance the water permeability to achieve an excellent filtration performance [109]. The purpose of sulfonation processes is to convert the polymer material into an ionomer and confers their protonic conduction properties in better hydrophilicity, selectivity, and increased solubility in processing solvents [110]. Generally, PPSU polymer has low proton conductivity values due to the no active protonic site that can transport protons through the polymer chain. Therefore,
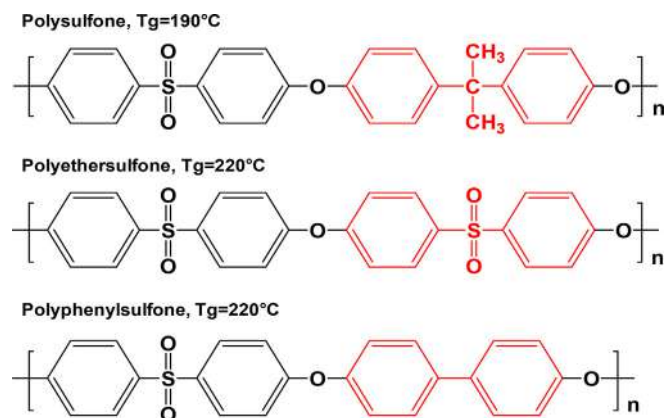
Fig. 5. Molecular structure of sulfone polymer. Reprinted with permission from Ref. [78]. Copyright (2011) Elsevier.

Table 1
Various applications of PPSU membranes.

Materials	Applications	Reference
PPSU/Silica	Plant-inspired dewatering system on pervaporation dehydration	[86]
Copper-1,3,5-benzenetricarboxylate-PPSU	Methanol separation	[87]
Activated carbon modified PPSU	Phenol adsorption	[88]
ZIF-8-PPSU	Gas separation	[89]
PSU/PPSU	Heavy metal rejection	[90]
PPSU-GO	BSA and pepsin rejection	[91]
PPSU/zeolite Socomy Mobil-5 (ZSM-5)	Organic component separation	[92]
PPSU/bismuth oxychloride nano-wafers	Oily wastewater separation	[93]
Carboxylated graphene oxide/PPSU	Nanofiltration membrane for heavy metal ion removal	[94]
SPPSU/hyperbranched polyethyleneimine	Organic solvent nanofiltration	[95]
PPSU/ZIF-8	Solvent-resistant nanofiltration	[96]
PPSU/CuO/graphitic carbon nitride	Protein separation for wastewater treatment	[97]
PPSU/silver-coated hydroxyapatite	Palm oil mill effluent treatment	[98]
SPPSU/PBI	Hydrogen purification	[99]
PPSU/SnO2	Ultrafiltration membranes for dye removal	[100]
PPSU/cellulose acetate	Ultrafiltration membrane for arsenic removal	[101]
PPSU/SPEEK	Vanadium flow battery	[102103]
PPSU/multiwalled carbon nanotubes	Heavy metal removals	[104]
PPSU	Biogas upgrading	[105]
Zwitterionic nanoparticles/PPSU	Protein rejection	[106]

the best approach to modifying PPSU for PEM application is to employ sulfonic acid groups on PPSU aromatic rings through the sulfonation process. This sulfonic acid group is capable of becoming a medium for proton transportation where it is easily can be attached to the PPSU polymer chain through sulfonation reaction. By introducing SO_3H groups within the polymer chain, ion exchange capacity, hydrophilicity, solubility in polar solvents, proton conductivity, and the transport number of sulfonated PPSU (SPPSU) significantly increased [99].

The proton transportation within the SPPSU membrane depends on the hydrated membrane, whereas a polymer matrix holds the water. Generally, two mechanisms for proton transportation happen in the PEM, which are structured diffusion and vehicle diffusion [111]. The structure diffusion of protons, also known as the Grotthuss mechanism, refers to the proton transportation by tunneling from one water molecule to another via hydrogen bonding known as "proton hopping". Proton hopping is the process of a proton (H^+ ions) through the network of hydrogen bonds. On the other hand, it should be noted that water has a high self-diffusion coefficient, which contributes to the total proton conductivity of protonated water molecules in the form of H_3O^+. In the Grotthus mechanism, proton diffuses from one hydrolyzed ion (SO_3^-, H_3O^+) to another through the polymer matrices. A water-free proton-conducting membrane with an active functional group for proton transportation will offer high proton conductivity under low humidity conditions considered to function by this mechanism [100]. Water-free proton-conducting membranes are more demanded in which the proton transportation lying under Grotthus-mechanisms can operate higher than the boiling temperature of the water. Yoshimura *et al.* [112] modified PPSU by adding a highly acidic semisquaric acid group so that the proton dissociating group can conduct proton by the Grotthus mechanism above the boiling point of water. The transportation of proton in this mechanism starts from the movements of hydronium ions by proton produced from hydrogen oxidized at the anode combining with the water molecules. Additional nearby water molecules will pull the proton from these hydronium ions, and the process will be repeated until the proton reaches the cathode side [113].

This occurrence can be called a vehicle diffusion in which it contributes approximately 22 % to the total conductivity [114]. In this mechanism, the maximum temperature used for the membrane is limited approximately to the boiling point of water that usually happen in the polymer without an active functional group for proton transportation. The electro-osmotic drag in the membrane becomes a medium for hydronium ions (H_3O^+) transportation that is transported through the aqueous medium with more water molecules that causing the water/methanol molecules to become a source for proton diffusion through the membrane [115]. Cationic complexes such as hydronium ions H_3O^+ are the results of a combination between proton and water. In the sulfonated PPSU polymer chain with -SO_3H functional groups become the carriers for proton transportation. These sulfonic acid functional groups increase the number of water molecules by forming hydronium ions H_3O^+ according to the vehicular mechanism of the proton transportation [116]. Kim et al., [117] presented a proposed mechanism inside their developed sulfonated PAES nanocomposite membrane with modified silica-phosphate (see Fig. 6). This nanocomposite membrane follows both transportation mechanisms that were detected from conductivity results. The high conductivity of the membrane is due to the hydrogen bonding between the bound water and the hydroxyl group of the silica-phosphate and sulfonate groups of the polymer chain that enhances the proton conductivity through the Grotthuss mechanism. Meanwhile, the slightly tortuous path through the membrane due to the presence of inorganic materials has reduced the
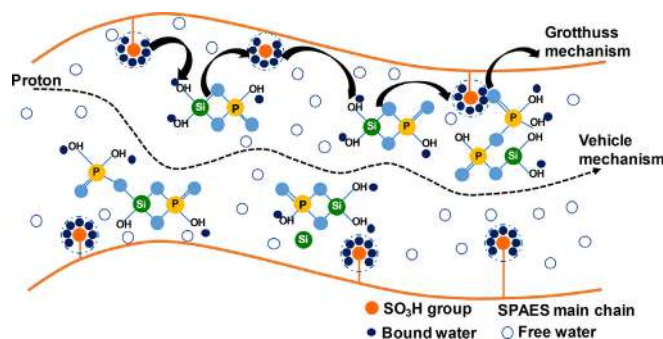

Fig. 6. Schematic diagram of the proton transport mechanism in the sulfonated (PAES)/silica-phosphate nanocomposite membrane. Reprinted (adapted) with permission from Ref. [117]. Copyright (2011) Elsevier.

membrane conductivity, following the vehicle mechanism for proton transportation.

In a sulfonation reaction, the degree of sulfonation is vital in determining the polymers' properties. The D.S can be well controlled by adequately selecting the sulfonating agent, concentration, reaction temperature, and reaction time. The sulfonating agent helps to enhance the reactivity of the sulfonation process. Generally, sulfonations for polymers can be conducted with sulfonating agents such as concentrated sulfuric acid, fuming sulfuric acid, sulfur trioxide complexes, chlorosulfonic acid, and acetyl sulfate that was chosen based on the reactivity of the polymers [118]. Concentrated sulfuric acid (95 % to 98 %) was the most used sulfonating agent to sulfonate the polymer. The direct linkage between aromatic moieties makes the PPSU structure more rigid, but at the same time, it offers two activated phenyl rings for the electrophilic aromatic substitution reaction. Furthermore, Liu *et al.* [119] reported that varying the concentration of sulfonating agents achieved different D.S for the PPSU polymers. Other than that, varying the reaction temperature and reaction time also results in different D.S. Parreño *et al.* [120] reported on the effect of varying the reaction time on the sulfonated polybenzoxazine (PBz) nanofibers. They stated that by varying the reaction time, the dimensional stability of the sample was affected and determined that the sample achieved different D.S values.

Consequently, it is easily possible to introduce two sulfonic acid groups per repeating unit (2nd substitution) in the PPSU molecular structure by adequately determining the optimized conditions during the sulfonation reaction. Di Vona et al., [121] present a study that they can develop two sulfonic acid groups in one repeating unit of PPSU by tuning the sulfonation reaction conditions using strong sulfonating agents with longer reaction times. Furthermore, Matsushita and Kim [122] also reported on the soluble SPPSU bearing two sulfonic acid groups in the PPSU polymer chain through similar sulfonation reaction conditions that are shown in Fig. 7(**a**). Meanwhile, Xing and Kerres, [74] prepare the sulfonation reaction of PPSU using the metalation route shown in Fig. 7(**b**). This preparation method also required optimized conditions to achieve the desired D.S for any applications.

The sulfonation of PPSU with SO_3H groups will lead to two fractions, water-soluble and highly sulfonated with D.S > 1.5 fractions and water-insoluble fraction with D.S < 0.7 concerning a number of sulfonic acid groups per monomer unit [123]. SPPSU with high D.S showed fewer tendencies to convert to coherent dry film due to highly soluble polymers in the water [124]. Investigation of the polymeric membrane with different D.S revealed that high D.S could improve the conductivity of the polymer membrane. Xiang *et al.* [125] reported that the varying conductivity values of sulfonated polyaryl ether ketones (SPAEKs) were achieved by
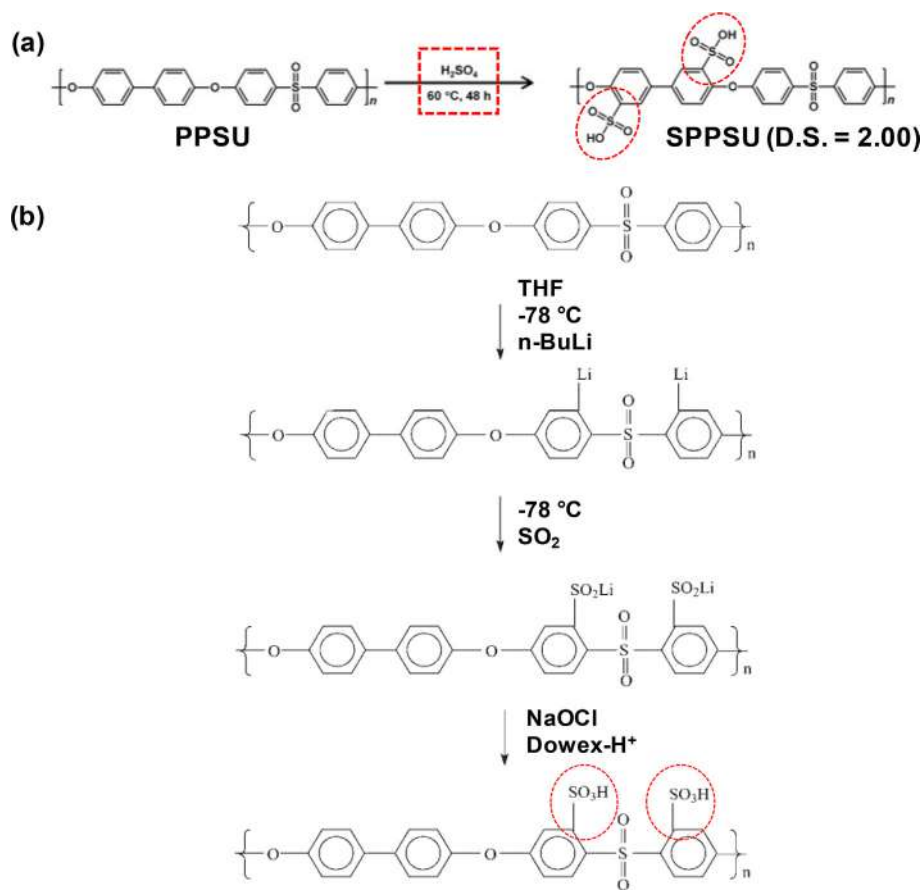
Fig. 7. Sulfonation synthesis for 2nd substitution for PPSU polymer (b) direct sulfonation using sulfonationg agent. Reprinted (adapted) with permission from Ref. [122]. Copyright (2018) Elsevier, and (c) sulfonation synthesis through metalation route. Reprinted (adapted) with permission from Ref. [74]. Copyright (2006) John Wiley and Sons.

Table 2
Summary of sulfonation conditions towards PPSU membrane properties.

Sulfonating agent	D.S./IEC	Mechanical strength	Proton conductivity	Remarks
- Concentrated H$_2$SO$_4$ Fuming sulfuric acid Sulfur trioxide complexes Chlorosulfonic acid Acetyl sulfate	Low Medium High	Good Good Weak	Very Low Low Very high	- Low protonic site for proton conduction - Proton conductivity is much lower as compared to perfluorosulfonic acid membrane - Unable to form a membrane Sulfonated PPSU is dissolved in water which require further treatments such as crosslinking, chemical modifications or composite with another materials

changing the sulfonation degree. They used SPAEKs with sulfonation degrees 0.4 to 1.0, and SPAEKs with 1.0 D.S. achieved the highest proton conductivity values that exceeded the conductivity of the tested Nafion® 117 membranes. On the other hand, Dyck *et al.* [123] also reported that SPPSU with 1.0 D.S results in high conductivity. It has been proven that the D.S plays a vital role in enhancing the proton conductivity of PEM [126]. The proton conductivity values of the SPPSU membrane are increasing along the degree of sulfonation. However, typically highly sulfonated with D.S > 1.5 fraction results in excess membrane swelling that contribute to failure mechanical and chemical durability of the PEM [127]. It is regrettable to sacrifice the potential of highly sulfonated PPSU polymers, which will contribute to the excellent proton conductivity as PEM due to the mechanical failure and chemical instability factors.

The properties of PPSU by sulfonation reactions are summarized in Table 2. According to the required properties, many researchers found that the crosslinking technique is one of the methods that

have been extensively studied. Generally, crosslinking can be easily defined as forming a covalent bond to join two polymer chains. Kulasekaran *et al.* [128] applied crosslink methods to crosslink between the poly (vinyl alcohol) and sulfonated polyethersulfone crosslinked through ether linkage PEM for fuel cell applications. The polymer chain becomes more rigid when undergoes crosslinking reaction and membrane durability increases [129]. The modifications of the sulfonated polymer membrane by multiblock copolymers and the possibilities of applying thermal crosslinking to improve the membrane properties were discussed.

PPSU modifications by multiblock copolymer

An exciting strategy to improve the PPSU polymers as a PEM is the synthesis of copolymers with tunable architectures. This block copolymer is composed of hydrophilic and hydrophobic channels leading to nanophase-separated domains with continuous proton-conducting channels. Generally, copolymers have lower

proton conductivity values at lower water contents due to the poor connectivity of the proton-conducting hydrated phase domain. This suggests that the development of the multi-block copolymers should have highly sulfonated segments with an excellent phase separation between hydrophilic parts to maintain the sulfonic acid concentration in the membrane [130]. Besides, excessive water uptake and mechanical deterioration should be avoided with a high relative humidity [131]. Currently, the researcher is focusing on building the micro phase-separated block copolymers with highly active sulfonated functional groups for efficient proton conduction at high operating temperatures and low relative humidity conditions. Multi-block copolymers comprise two or more homopolymer repeat units linked by covalent bonds. An approach to enhance the proton conductivity values at a higher temperature and low relative humidity conditions is to induce the distinct phase separation between the hydrophilic and hydrophobic domains through block copolymers architectures with stable mechanical properties. Lee et al., [132] developed the multi-block copolymers consisting of hydrophilic hydroquinone and hydrophobic PAES, which achieved high proton conductivity ranging from 13.0×10^{-2} to 21.0×10^{-2} S cm^{-1} and good mechanical properties. Generally, the open circuit voltage (OCV) measurement is closely related to the fuel and oxidant crossover through the membrane. Without applying any current, the OCV measure was ideally about 1.23 V, which indicates that the higher OCV is related to excellent PEM durability towards the fuel and oxidant crossover. The excellent phase separation of hydrophilic and hydrophobic segments in the multi-blockchain has also been shown to reduce the hydrogen crossover that shows higher OCV, which was very important to sustain the prolonged operation of the fuel cell system [133].

Kim et al. [134] introduce the 3,3′, 5′5′-tetramethylbiphenyl-4, 4′-diol with four bromination sites and bis (4-chlorophenyl) sulfone as a hydrophilic site to build the multi-block copolymers PAES for the AEMFC cell system. The multi-block copolymers have shown an improvement in the hydroxide conductivity as well as alkaline stability. Although the OCV data was not included in the manuscript, it can be predicted that the OCV is high due to the high-power voltage measured by the small current density reported in the study. The membrane also shows stable power density and voltage up to 18 h, which remarks the membrane properties durability towards fuel crossover and chemical degradation. Lee et al. [82] developed hydrophilic-hydrophobic multi-block copolymers based on PAES polymers for PEMFC applications. Due to their well-separated microstructure, the proton conductivities were improved, supporting well-connected hydrophilic domains in the copolymers chain. The result is consistent with the report by Titvinidze et al. [135], where the multi-block copolymers of hydrophilic SPPSU and hydrophobic PES segments show high proton conductivity with superior hydrolytic stability. Jung et al. [77] developed a series of multi-block copolymers containing sulfonated poly(arylene sulfone) (SPAS) blocks to achieve high proton conductivity and excellent durability in fuel cell systems under various RH conditions.

Consequently, the multi-block polymers showed excellent hydrogen crossover performance under low humidity conditions with outstanding durability. The OCV hold a test for more than 1400 h (see Fig. 8(**a and b**)). OCV hold test was measured to determine the chemical durability of the membrane since, under extremely low humidity condition, the harmful peroxide will be generated through the diffusion of H$_2$ and O$_2$. This peroxide will result in rapidly degrade the PEM that leading to membrane pinholes, thus increasing the H$_2$ crossover. Ureña et al. [136] developed multi-block copolymers composed of PSU and PAES by polycondensation in a one-pot, two-step synthesis. With the high D.S (0.98 to 1.58), this nanocomposite polymer membrane achieved proton conductivity up to 0.03 S cm^{-1} at 70 °C with excellent thermomechanical stability.

Rowlett et al. [137] investigated the properties of PEM-based multi-block copolymers consisting of Nafion copolymers that served as a hydrophobic segment and a block of SPAES as a hydrophilic segment (6FPAEB-BPSH) (see Fig. 8(**c**)). It shows that the water uptake and IEC of the membrane were greatly enhanced, contributing to improving the proton conductivity. This property can be achieved by controlling the length of the SPAES block that serves as a hydrophilic contributor. Excessive swelling was reported with longer SPAES block lengths unsuitable for PEM. Afterwards, they reported on the capability of this multi-block copolymer membrane in MEA and subsequent fuel cell testing [138]. Fig. 8(**d) and (e)** shows the polarization of 6FPAEB-BPSH membrane testing at a different level of relative humidity conditions and commercial Nafion 212 membranes as a reference to compare the results. At higher RH conditions, 6FPAEB-BPSH membranes show similar performance to the Nafion membrane at lower current density (up to 0.8 A cm^{-2}), whereas Nafion showed a sharp voltage drop at higher current density. Meanwhile, 6FPAEB-BPSH shows slightly low performance compared to Nafion, which might be due to the poor compatibility between 6FPAEB-BPSH with Nafion ionomer on the electrodes. Although Nafion is still showing excellent performance, the outcome performance of 6FPAEB-BPSH multi-block copolymers in fuel cell systems can be further improved with some modifications to the interfaces between the membrane and the electrodes, lead to better cell performance. Well define hydrophilic domains that are derived from the well hydrophilic and hydrophobic separation are needed for an efficient proton conductivity [133]. In this case, the modification of the PPSU using multi-block copolymers with well hydrophobic and hydrophilic phase separation will utilize the facile proton transportation along the distinctively hydrophilic phase that will be contributed to better cell performance. Although the multi-block copolymer is one of the modification ways for PPSU-based-PEM, complex chemicals are needed to construct the well-defined microphase separated by hydrophobic and hydrophilic channels. The previously reported study regarding modifications of PPSU by multiblock copolymer was summarized in Table 3.

Modifications of highly sulfonated PPSU membrane by thermal crosslinking

Improvements in the thermal, mechanical, and physicochemical properties of the polymers used are crucial challenges in polymer synthesis and the quest for new search applications. The properties of polymeric materials depend on their chemical nature. Still, they also depend on their molecular weight and the function of the polymer chain for a given polymer type. PEM-based engineering thermoplastic polymers are now considered a proven technology and widely used in a broad range of applications. However, there are still challenges to making it comparable with the commercially Nafion membranes [141]. The alternative membranes include maintaining membrane performance, thermal stability, and chemical resistance under continuous operating conditions. According to the mechanical failures of the highly sulfonated membranes, the crosslinking techniques offer the best option to counter the problems. In polymer chemistry, the resulting mechanical properties of the crosslinking polymer are highly dependent on crosslink density. Low crosslink density will only increase the viscosities of the melting polymer, while intermediate crosslink density transforms gummy polymers into materials with elastomeric properties and potentially high strengths. Very high crosslink densities will result in very rigid or glassy materials [142]. The crosslinking will provide many benefits to the polymer matrix, such as higher
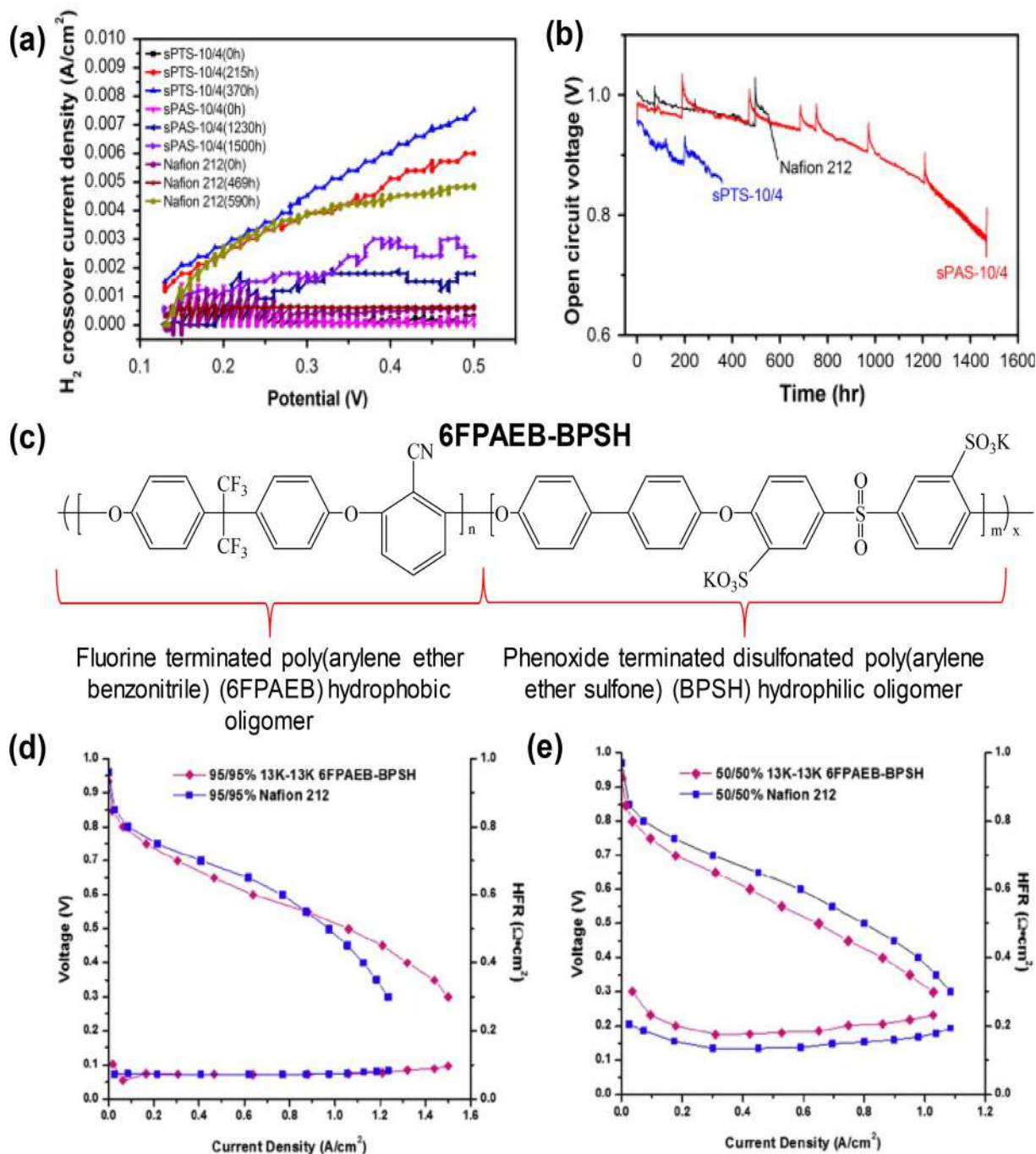
Fig. 8. (a) Variation of hydrogen crossover current density for H_2/N_2 and (b) durability comparison under OCV testing at 80 °C and 10 % RH conditions for SPAS block copolymers. Reprinted with permission from Ref. [77]. Copyright (2014) Elsevier, (c) structure of multiblock hexafluoropropane poly(arylene ether benzonitrile) disulfonated poly(arylene ether sulfone) copolymers (6FPAEB-BPSH), and polarization curve of the 6FPAEB-BPSH and Nafion® 212 MEAs at (d) 95 %/95 % and (e) 50 %/50 % relative humidity conditions. Reprinted with permission from Ref. [137,138]. Copyright (2013, 2017) Elsevier.

tensile strength, resistance to stress cracking, no electrical charge, negligible difference in thermal stability, decreased flexibility and improved high-temperature mechanical [143]. Crosslinking has received much attention since it appears to provide a promising approach to enhancing chemical and thermal resistance. Crosslinking modification can be achieved by thermal or chemical crosslinking, further discussed in the next section. Crosslinking reactions are among the most powerful ways to control and improve polymeric materials, such as swelling and mechanical behaviour. However, reticulation often relies on introducing the crosslinker species, which requires special procedures such as grafting by irra-

diation. Harilal et al. [24] report on the crosslinked PBI membrane for PEMFC using brominated polyphenylene oxide as a crosslinker, and crosslinked membrane shows many improvements in chemical stability, mechanical strength, and strong resistance to membrane swelling in concentrated acidic solutions. Generally, the high proton conductivity of PEM with high IEC and D.S usually leads to large dimensional variation and low mechanical strength.

The cross-linking method becomes the most straightforward solution to the problems as it effectively controls excessive membrane swelling. An et al. [127] reported using gradient crosslinking to crosslink the SPEEK membrane by immersing it in sodium

Table 3
PPSU modifications through multiblock copolymers in fuel cell applications.

Composite membrane	Conductivity (S cm^{-1})	Mechanical strength (MPa)	Elongation at break (%)	Water uptake/ swelling RT (%)	Power density (mW cm^{-2})	Temperature (°C)	RH (%)	Type of fuel cell
Multiblock copolymers SPAES[77]	0.028, 80 °C, 50 % RH	9.0	24.0	58.0/20	495.6	70	50	PEMFC
Block copolymers PES/PAES[134]	0.0518, 90 °C, 100 % RH	-	-	45.0/29.6	64	60	100	AEMFC
PAES multiblock copolymers/butanesulfonic acid-ethanedion groups[130]	0.171, 80 °C, 65 % RH	50.62	13.8	14.4/15.7	424.8	60	100	PEMFC
Multiblock SPPSU/SPSU[136]	0.0341, 70 °C, 95 % RH	55	57	23.9/-	~400	70	100	PEMFC
Multiblock poly(arylene ether nitrile) disulfonated PAES copolymers[137,138]	0.140, 80 °C, 95 % RH	50–60	11–16	51/-	~520	80	95	PEMFC
Multiblock SPAES/SPP[23]	0.102, 70 °C, -% RH	-	-	69.5/-	630	80	100	PEMFC
Partially fluorinated Multiblock SPPSU[139]	0.340, 80 °C, 90 % RH	-	-	31/-	292.8	80	80	PEMFC
Multiblock copolymers sulfonated PPSU/ imidazolium PPSU[140]	0.086, 80 °C, -% RH	59 ± 3	52 ± 3	~34/43	60.11	80	-	DMFC

borohydride and sulfuric acid solutions. The simultaneous diffusion and reaction of sodium borohydride with reduced SPEEK ionomers result in no damage to proton conductance but effectively controls the membrane swelling and improves mechanical strength. Occasionally, crosslinking can modify the properties of the polymer membrane, such as increased membrane water uptake, inducing brittleness, and even reducing the proton conductivity [144]. The crosslinked membrane can become brittle, and the formation of a proton channel inside the membrane can be disrupted. Furthermore, the proton-bearing sulfonic acid group in the ionomers was sacrificed during crosslinking, which usually decreased proton conductivity values. A study by Feng et al. [145] describes the effect of crosslinking time and Araldite MY721 epoxy resins crosslinker concentration on hydroxyl-functionalized SPEEK. It shows that a longer reaction time results in membrane water uptake and proton conductivity values and reduces the methanol swelling ratio compared to the pristine SPEEK membrane. Increasing in the epoxy resin concentration has tremendously decreased the methanol permeability. During the crosslinking reaction, the optimized condition showed a proton conductivity of ~0.096 S cm^{-1}, which meets the requirement for PEMFC (0.1 S cm^{-1}).

Besides, the degree of crosslinking plays a vital role in the optimized properties of the sulfonated polymer. The desired dimension of the crosslink polymers is hardly to be maintained by having high IEC values with a too low degree of crosslinking. On the other hand, larger crosslinking degrees resulted in membrane brittleness and decreased proton conductivity, which has restricted the application of the polymer membrane to be applied in fuel cell applications [144]. Zheng et al. [146] reported the effect of crosslinking degrees on sulfonated poly (aryl ether nitrile) using an allyl bisphenol A crosslinker. They reported that an increase in crosslinking degrees had enhanced the tensile strength of the crosslinking membrane but reduced IEC and proton conductivity values. It is suggested to optimize the crosslinking reaction conditions such as crosslinker, crosslinker concentrations, crosslinking time, and crosslinking temperature. The thermal crosslinking process is time and temperature dependent. To crosslink the polymer chain, the polymers are heated below their glass transition temperature (T$_g$) to relieve the internal stresses introduced during the fabrications [147]. Thermal crosslinking of ion-conducting polymers decreases the free volume between the polymeric chains, thus inducing a mechanical stabilization of polymeric materials [143]. Thermal crosslinking can play a crucial role in changing membrane morphology. Thermal treatment lower than T$_g$, the polymer chains are mainly fixed, thereby maintaining the existing morphology.

Unfortunately, at higher than T$_g$, the polymer chain becomes lessened, resulting in changing the physical properties of the polymers [146]. Joseph et al. [148] prepared the crosslink PBI/sulfonated polysulfone-based blend membranes (see Fig. 9) by introducing the thermal crosslinking step to avoid the N-CH$_2$ links reduce the membrane conductivity and simultaneously improve the mechanical stability of the membrane. The chemical, thermal and mechanical stability of the thermally crosslink PBI with SPPSU was also improved and potentially used in high-temperature PEMFC and has been proven by other reported studies [147,149].

A part of sulfonic acid groups of highly sulfonated polymers can be sacrificed to perform further functionalization, such as crosslinking without a sensible loss in electrochemical performances. A sulfonated polymer can be crosslinked under thermal treatment at a specific temperature through bonding between sulfonic acid groups. The crosslinks via sulfone bridges (SO$_2$) can be achieved by one-step condensation reactions of sulfonic acids attached to the polymer chain, triggered by heat treatment without being introduced to the crosslinker [150]. The first report about the thermal crosslinking reaction claimed that the thermal treatment of SPEEK was assumed to occur at 120 °C [151]. The development of cost-effective and straightforward thermal crosslinking treatments assisted by a polar aprotic solvent such as DMSO enhances the stability and performance of SPEEK. It was demonstrated that after treatments performed in air at temperatures higher than 160 °C, crosslink SPEEK membranes result in higher mechanical strength than the uncrosslinked SPEEK membrane and could resist water up to 145 °C without significant swelling [152]. Moreover, Joseph et al. [148] crosslink polybenzimidazole by applying heat over 200 °C and developing a membrane with higher gas tightness and good cell performance.

Maranesi et al. [153] have depicted the possible pathways for crosslinking via SO$_2$ bridges under a thermal crosslinking reaction illustrated in Fig. 10. They reported three possible ways in the formation of crosslinking SPEEK. First, the attack is activated free if the SPEEK has D.S lower than 1 (pathway a). Next is the attack in the deactivated ring in the meta position of sulfonic acid groups or carboxylic acid groups (pathway b). Pathway c shows the electrophilic species' attack in the aromatic ring's position, where the sulfonic acid groups are present (high D.S polymer). The D.S = 1.0 of the SPEEK heated at 120 °C was obtained by titration, and elemental total sulfur analysis was then further treated at 180 °C for 15 h. After the second treatment, the titration gave results of D.S = 0.6, that is, 0.6 mol of sulfonic acid groups, for one repeating unit. The D.S reduction suggests that crosslinks form between sulfonic acid groups and eliminate some sulfonic acid groups. The
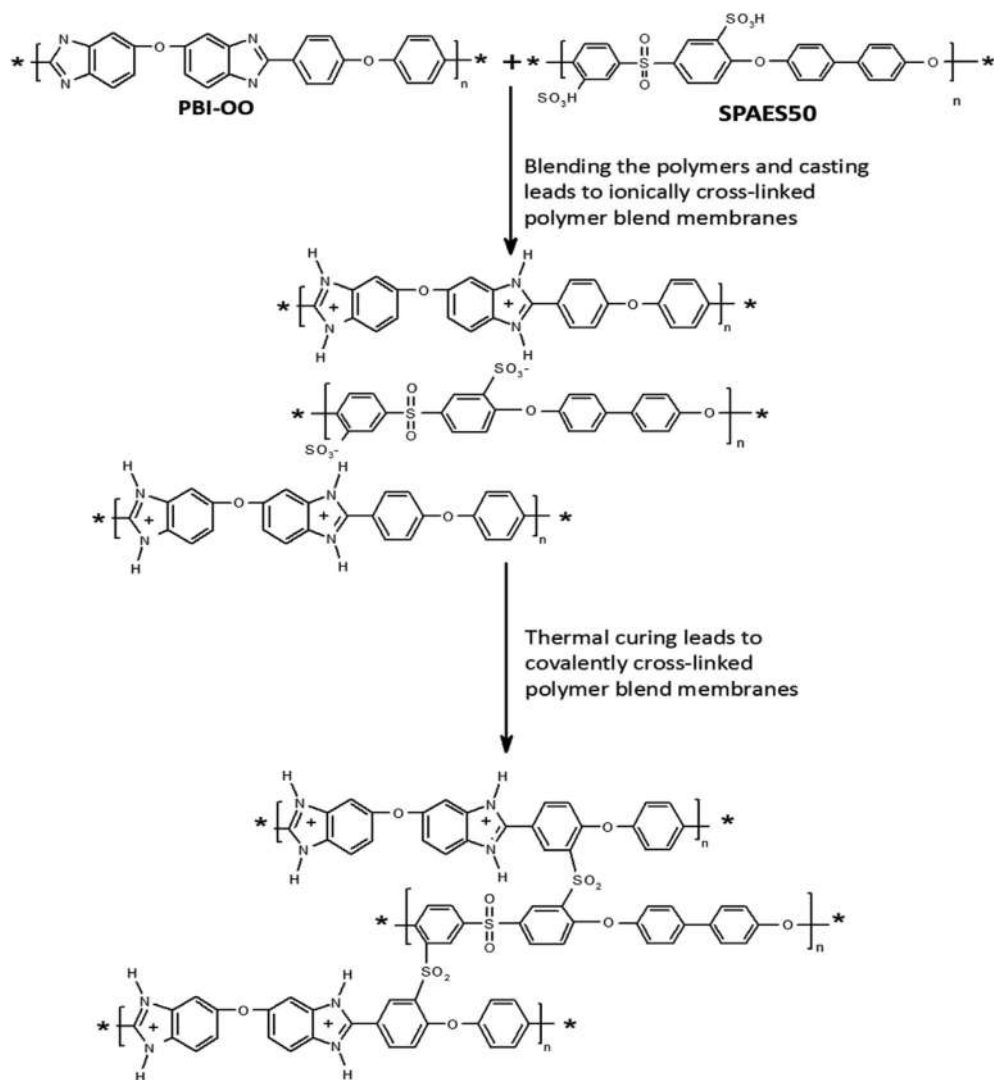
Fig. 9. The scheme for the crosslinking reaction between PBI and SPPSU. Reprinted with permission from Ref. [148]. Copyright (2017) Royal Society of Chemistry.

approach using thermal crosslinking without incorporating a crosslinking agent, often sensitive to the operating conditions, is merely realizable and suitable for all D.S values [154,155].

The incredible impact on the polymer crosslinking by sulfonic acid bridges between macromolecular chains of SPEEK through the thermal crosslinking process was further reported on other aromatic polymers. Wu *et al.* [156] applied thermal crosslinking to crosslink that sulfonated poly (2, 6-dimethyl-1,4-phenylene oxide) (SPPO) under different times and temperatures. The SPPO membrane prepared at 80 °C for 5 h results in high proton conductivity and excellent mechanical properties. Meanwhile, Kim *et al.* [117] applied thermal crosslinking on the sulfonated polyethersulfone (SPES, D.S = 1) and highly sulfonated PPSU (SPPSU, D.S = 2) for fuel cell applications. The effect of thermal crosslinking on SPPSU was further reported [31]. The crosslinked membrane resulted in water-insoluble properties upon heating at 180 °C. This method was further applied to SPPSU with high IEC. The produced membrane shows an excellent thermal and mechanical stability [157]. The results were consistent with Kim *et al.,* [150] on the 2nd substation sulfonic acid groups on the SPPSU polymer matrix. It indicates that thermal crosslinking can be applied to a wide variety of aromatic sulfonated polymers that apply to a wide range of IEC values. This method is economically preferable, upscale, and thus suitable for practical applications. The possible crosslinking struc-

ture of SPPSU with 2nd substitution sulfonic acid is illustrated in Fig. 11. This straightforward technique to improve the mechanical and thermal properties of the membrane are potential can be improved by studying the properties of the membrane along the heating process and optimize conditions in applying thermal conditions should be reported. Although crosslinking offers an option to improve the mechanical strength of the membrane, the sulfonic acid functional group proton transportations were also reduced. This results in reducing the proton conductivity of the PEM. One of the techniques to keep maintaining the proton conductivity of the highly sulfonated membrane with improved mechanical properties is the addition of composite materials. Some studies reported on applying the highly sulfonated PPSU polymers but with the addition of nanomaterials to counter the drawbacks of failure. Nor *et al.* [28] reported the effect of incorporating thermal crosslinking carbon nanodots (CND) towards improving the proton conductivity of the sulfonated PPSU with D.S ~2 fraction. The incorporation of CND into the SPPSU membrane shows superior dimensional stability and even enhances the membrane's proton conductivity under low relative humidity conditions. The remarkable performance of the PPSU base polymer as a potential PEMs has directed an extensive effort to develop a variety of attempts to prepare a more stable PPSU-based PEM with various modifications. The modifications of the SPPSU by modifying it with various com-
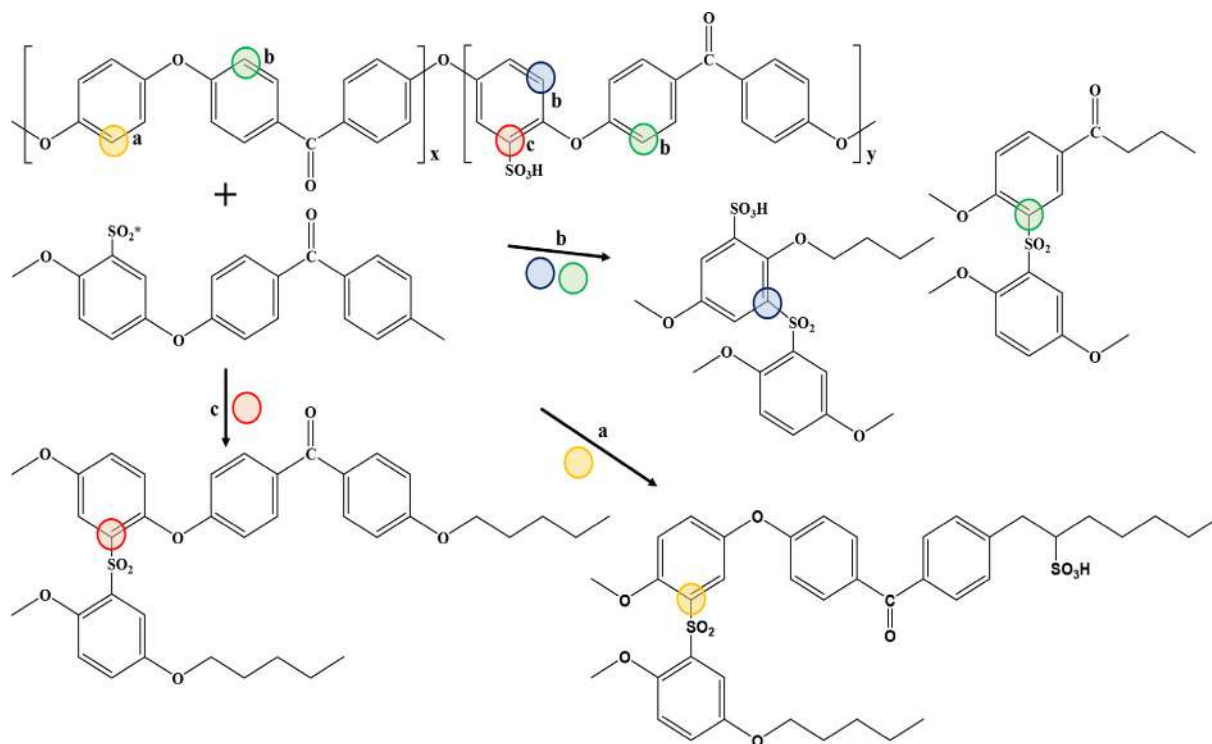
Fig. 10. Possible pathways for crosslinking reaction via SO$_2$ bridges in SPEEK polymers. Reprinted with permission from Ref. [153]. Copyright (2013) John Wiley and Sons.
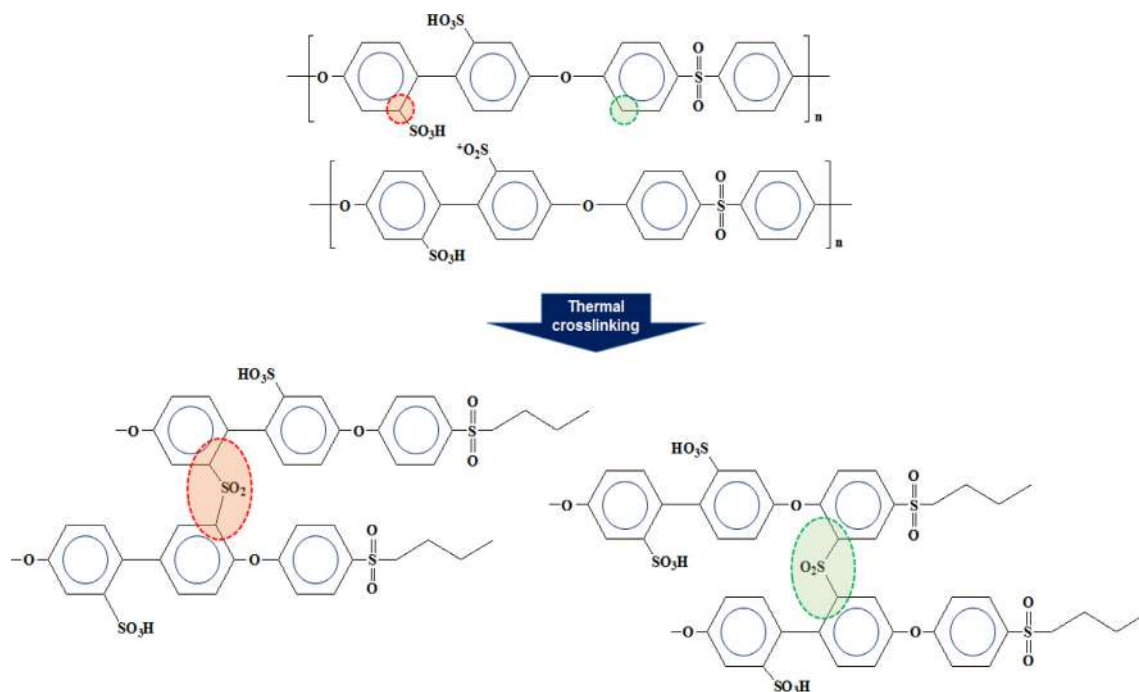

Fig. 11. Possible crosslinking products of SPPSU polymers. Reprinted with permission from Ref. [31]. Copyright (2016) Elsevier.

posite materials and improved properties of the composite SPPSU were discussed in the next section.

Modification of SPPSU proton exchange membrane with nanomaterials addition

Composite materials are a multi-phase combination of two or more component materials with different properties and forms

through compounding processes. It maintains the main characteristics of the original component and shows a new character not possessed by any of the original components [158]. While preparing the nanocomposite membrane, some factors must be considered depending on fillers and polymer backbone. The first consideration while preparing the nanocomposite membranes is the loading of the filler. Sahu *et al.* [159] reported on the properties of Nafion by incorporating various loading of sulfonated graphene (0.5 %, 1 %, 1.5 % and 2 %). It shows that incorporating 1 % sul-

fonated graphene achieved five times higher proton conductivity than the pristine Nafion membrane. By contrast, incorporating more than 1.5 % of sulfonated graphene reduces the proton conductivity values due to the excess amount of graphene that could disrupt the continuity of the proton conduction path. The optimum degree of filler loading should be achieved to prevent deterioration in the mechanical integrity of the membranes and block the proton conduction mechanism. Next are the filler size and distribution in the polymer matrix. The non-uniform distribution will lead to particle agglomeration that results in mechanical failure due to a disruption in the homogeneity of the polymer film. The filler particle distribution is affected by the chemical interactions between the polymer and the particles, the particle dimensions, and the dispersion of the fillers in the casting solvent [160]. Scipioni et al. [161] mentioned that a smaller tin oxide filler size had promoted enormous water affinity that contributes to the more regular organization of the polymer ionic channels in their research. Not restricted to that, it also increased the storage modulus of the Nafion nanocomposite membrane for better mechanical stability. The filler structure is one factor that can be considered while developing the nanocomposite membrane. Di Noto et al. [162] reported using the core–shell zirconia oxoclusters incorporated into the Nafion membrane matrix for low relative humidity fuel cells. It shows that core–shell zirconia oxoclusters result in better water retention at lower humidity conditions.

Nanocomposite membranes are attracting a great deal of attention to increase the temperature tolerance of conventional PEM materials. The objectives for the development of the nanocomposite membrane include several modifications like improving self-humidification of the membrane, reducing electro-osmotic drag and fuel crossover, improving mechanical strength without deteriorating proton conductivity, enhancing proton conductivity, improving the chemical and decomposition of the polymer backbone, also enhanced water retention capability at all operating temperatures and hydration state [134]. The oxidative and chemical stabilities of the sulfonated hydrocarbon membranes are not as good as perfluorosulfonic acid membranes because hydroxyl radical easily attacks hydrocarbon polymer. Therefore, the hydrocarbon polymer membrane has a short lifetime due to membrane degradation because of the hydroxyl attack. Deng et al. [163] reported using a confined perfluorosulfonic acid membrane that incorporated a water-stable metal–organic framework (ZIF-8 and MIL-101) as PEM. It shows that the nanocomposite membrane improves the water uptake and chemical stability of the nanocomposite membrane, and the MEA shows better cell performance under dry feed conditions. Park et al. [32] reported on nanocomposite Nafion with PPSU, whereas the PPSU is needed for mechanical reinforcement and controlling membrane swelling. Moreover, the introduction of metal–organic frameworks contributes to the water retention layer for water adsorption generated from cell reactions. Micro-phase-separated morphology with nanochannel has been formed to improve proton conductivity by blending ionomeric polymers with organic/inorganic hybrid materials. Many modifications have been successfully developed on PPSU-based PEM. Among them is integration with different types of additives such as carbonaceous nanomaterials, silica, inorganic clay and a metal oxide that was discussed in the next chapter.

Carbonaceous materials

Carbon can be found in nature through its elemental form as graphite, diamond and coal, which are the most abundant materials found on earth. The unique hybridization properties and sensitivity to discomposure during material synthesis make the carbon allotropes can be manipulated into fine nanomaterials, which has been extensively studied [164]. Notably, carbon can be found in

different hybridization states that have unique properties in which the chemical, thermal and electrical properties directly correlate to their structure that is widely used in several applications [165]. Carbon-based nanomaterials such as carbon nanodots, carbon nanotubes, graphene, graphene oxides, and fullerenes are attractive fillers used to develop various nanocomposites for PEM. In a study by Vani et al. [166], sulfonated carbon nanotubes were incorporated into polyvinyl alcohol to enhance the mechanical stabilities of the nanocomposite PEM. Meanwhile, Sun et al. [167] report on the properties of crosslink SPEEK nanocomposite doped with different carbon-based materials (graphene oxide and carbon nanotubes) or fuel cell applications. The doped 2D nanosheets graphene oxide exhibit higher proton conductivity and dimensional stability. Carbon nanotubes (CNT) are also attractive fillers for developing a variety of nanocomposite-based PEM. CNT is outstanding among a one-dimensional tubular nanofiller due to its excellent thermal, mechanical, and electrical properties. Unfortunately, CNT is heavily entangled because the strong Van der Waals force makes it difficult to disperse the polymer matrix [168]. CNT further underwent surface modifications to improve interaction with the parent polymer matrix. CNT functionalized with polydopamine (PDA) was incorporated into the chitosan polymer membrane to investigate the nanocomposite membrane's microstructure, membrane durability, and proton conductivity to be used as PEM in fuel cells. The proton conductivity improved by 33.3 % compared to the pristine chitosan membrane with exceptional thermal, mechanical, and oxidative stability [30]. Liu et al. [169] used multiwalled CNT as a filler in the Nafion membrane resulting in an increase of 1.5 folds of mechanical strength and a fivefold increase in proton conductivity.

Besides CNT, graphene is a carbon-based material that can be viewed as a one-atom-thick sheet of graphite. It has been investigated intensively in recent years due to its unique electronic properties. High-quality graphene sheets are often prepared by chemical vapor deposition, which requires expensive equipment. Graphene oxide (GO) was used instead to prepare graphene-like materials [170]. Indeed, graphene oxide can be reduced in solution and as a thin film using various reducing conditions that can convert graphene oxide into a material with a considerable enhancement in the electrical conductivity [171]. Besides, sulfonated graphene oxide incorporated into the Nafion membrane was reported for high temperature and low humidity PEMFC. The nanocomposite membrane achieves 4.74-fold higher proton conductivity than the pristine Nafion membrane at 120 °C under 20 % RH [64]. Lee et al. [172] introduced sulfonated poly(arylene thioether sulfone)-grafted GO (SATS-GO) nanocomposite in sulfonated PAES for PEMFC. The incorporation of GO into the SPAES matrix significantly contributed to high water uptake and chemical stability compared to the pristine SPAES membrane. The oxidative stability of the nanocomposite membrane was tested using the Fenton reagent, where all the nanocomposite membranes exhibited better oxidative stability than the pristine membrane. The introduction of SATS polymers grafted onto GO has significantly improved the interfacial interaction with the SPAES molecule, as there are no agglomerated domains were found in the cross-sectional SEM images of the nanocomposite membrane **(see** Fig. 12**(b–d))**. However, the incorporation of hydrophilic SATS-GO increased the IEC values of the nanocomposite membrane, which resulted in reducing the oxidative stability of the membrane (see Fig. 12**(e)**), where t_1 time elapsed for the membrane to start to break and t_2 dissolve completely. Meanwhile, Han et al. [173] reported on the performance of SPAES nanocomposite membrane bearing sulfonated polytriazole grafted graphene oxide (SPTA-GO) for PEMFCs. Incorporating the SPTA-GO has shown tremendous effects on the SPPSU membrane properties. Even though this nanocomposite membrane shows a higher water uptake, the
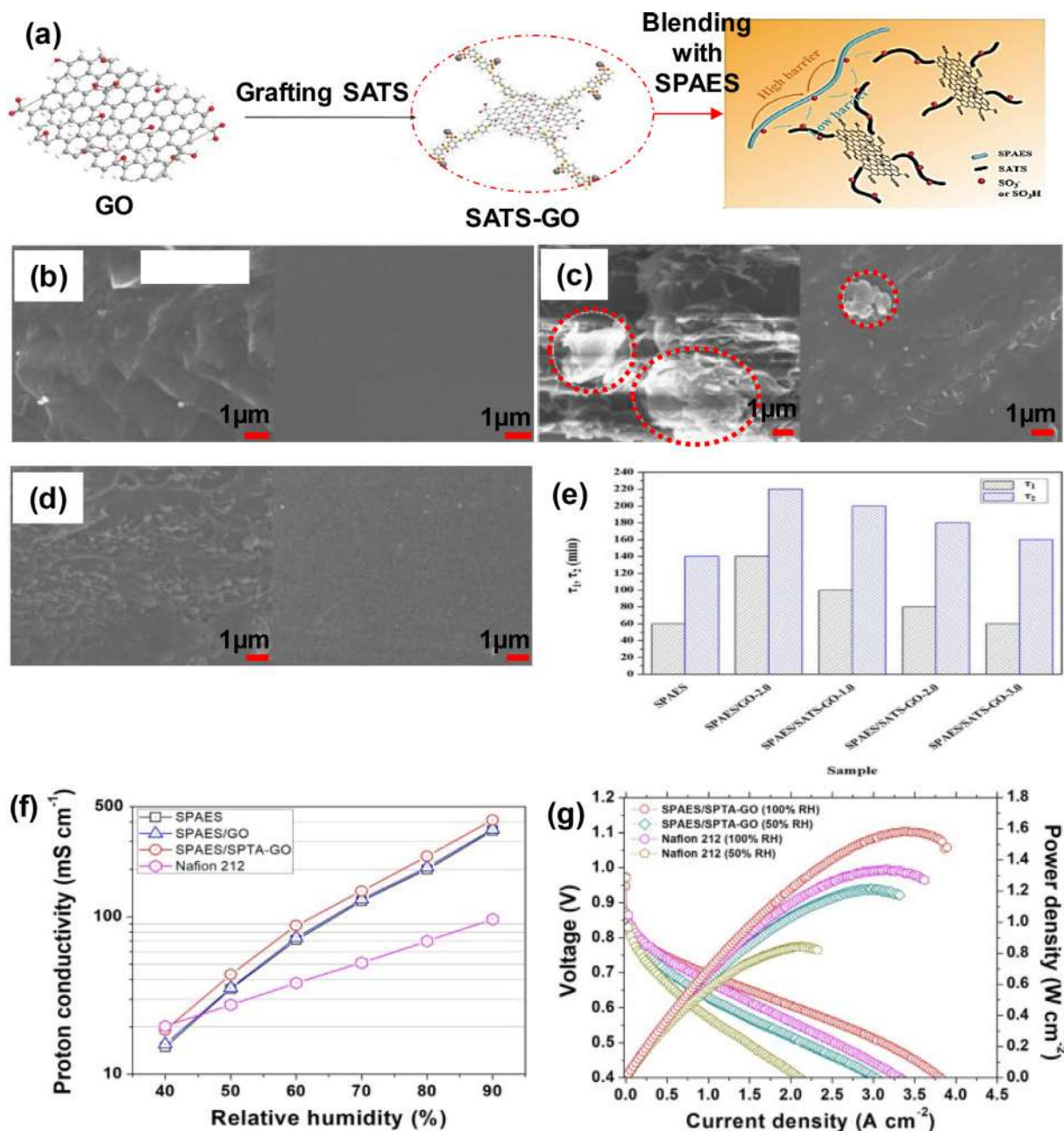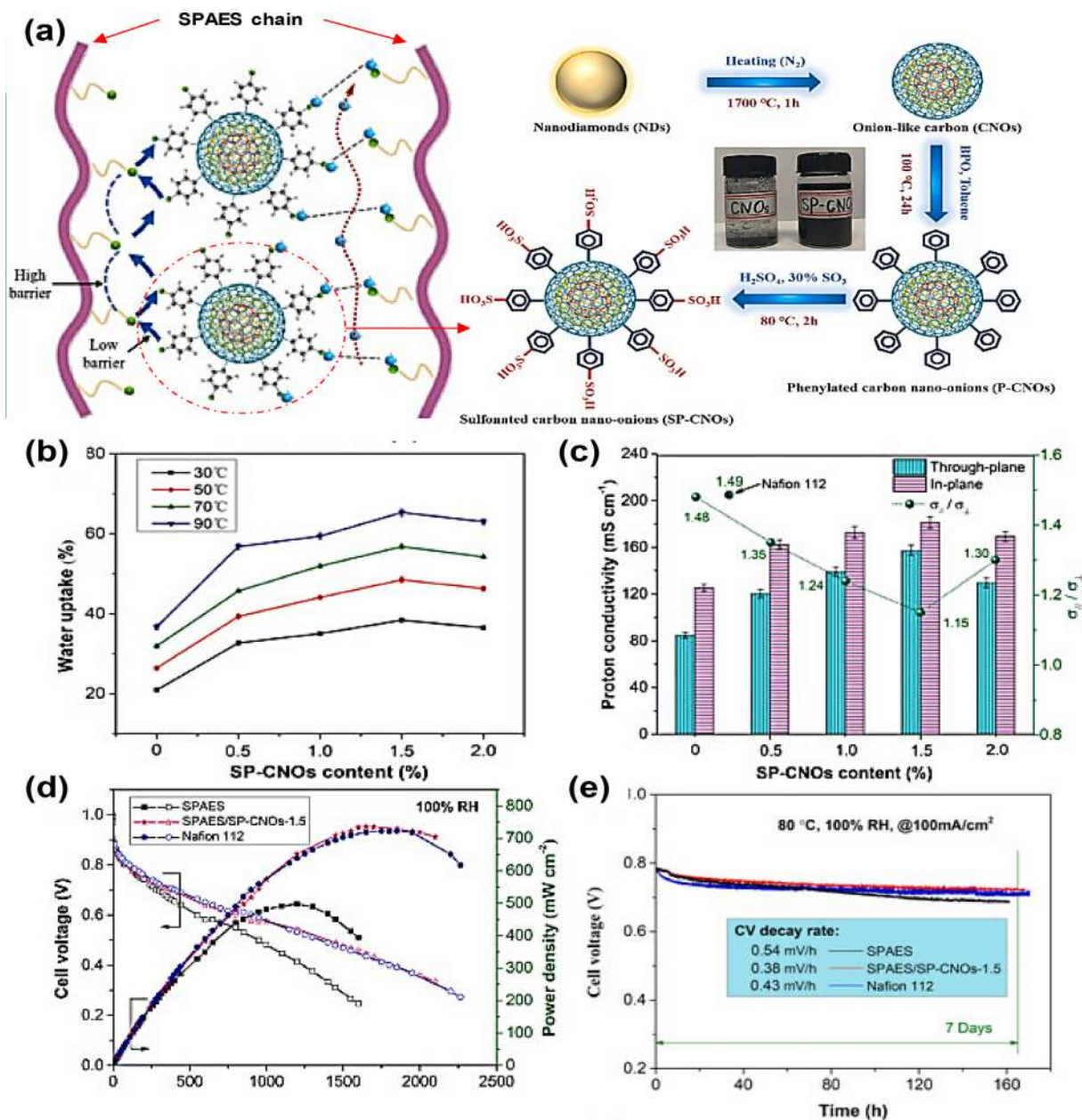
Fig. 12. (a) Schematic illustration of the SPAES/SATS–GO, the structure of GO and SATS–GO, SEM images of the (b) pristine SPAES membrane, (c) SPAES/2.0 GO, (d) SPAES/SATS–GO–1.0 and (e) chemical stability of the composite membrane. Reprinted with permission from Ref. [172]. Copyright (2019) Elsevier, (f) the proton conductivity membrane of SPAES, SPAES/SPTA–GO and Nafion 212 membrane at 80 °C under various %RH conditions (g) single-cell H_2/O_2 performance of SPAES, SPAES/SPTA–GO and Nafion 212 membrane at 80 °C. Reprinted with permission from Ref. [173]. Copyright (2020) Elsevier.

dimensional and chemical stabilities were superior compare to the pristine SPPSU membrane. The proton conductivity and fuel cell performance also are greatly enhanced and even show remarkable performance as compared to the commercial Nafion 212 membrane (see Fig. 12(**f and g**)). On the other hand, Lim and Kim [174] reported on the modified GO with perfluoropolyether group grafted onto GO (PFPE-GO) to evaluate the effect on SPAES and perfluorosulfonic acid (PFSA) membranes for PEMFC. From this report, the incorporation of PFPE-GO did not significantly impact the proton conductivity of the polymer membrane. However, it was found as a strategic solution to improve the mechanical and dimensional stability of the membrane with only a small amount of the PFPE-GO nanoparticles.

Carbon nanodots (CND) is an emerging new class of nanomaterials with a very small particle size which is about below 5 nm that have excellent property such as good conductivity, chemical inertness and excellent water solubility that are suitable to be incorporated into membrane based PEM [175]. The research publications on CND have been exponentially growing since 2006 due to the exclusive optical properties of CND compared to other types of carbon-based materials. Simple synthesis, low cost, vast precursors, excellent biocompatibility, and tunable surface properties make CND desirable to be developed. The state-of-the-art features have turned the CND into filler in the polymer-based electrolyte membrane for fuel cell applications. Jia *et al.* [176] introduced CND in the Nafion membrane structure to achieve high proton

Fig. 13. (a) The schematic illustration of proton transfer within SPAES/CNOs nanocomposite membrane and preparation route for sulfonated CNOs, (b) the water uptake and (c) proton conductivity of the nanocomposite membrane with different loading of CNOs nanofiller, (d) the polarization curve and (e) durability test of cell voltage under constant current density at 100 mA/cm² for pristine SPAES, SPAES with 1.5 wt% of CNOs and Nafion 112 membranes. Reprinted with permission from Ref. [177]. Copyright (2021) Elsevier.

conductivity and reduce the methanol permeability of the Nafion membrane for DMFC applications. The open circuit voltage of the nanocomposite membrane is higher than the pristine Nafion membrane, indicating that low methanol crossover the nanocomposite membrane during the DMFC testing. The Nafion/CND membrane effectively enhances the high-temperature water retention ability and proton conductivity values and reduces methanol permeability.

Nor et al. [28] developed SPPSU/CND nanocomposite membranes to see the potential in PEM fuel cell applications. The incorporation of CND has significantly improved the membrane flexibilities, water uptake and proton conductivity. The open circuit voltage (OCV) of the nanocomposite membrane measured was near to ideal OCV, which is 1.23 V, indicating that the nanocomposite membrane has high durability toward H_2 and O_2

crossover. CND also exhibit an excellent water solubility property that can promote efficient water retention ability that can facilitate large channel number for proton transportation. This zero-dimensional nanoparticle, like CND, offers a higher surface area and more active sites for the reaction, providing better interfacial compatibility with the polymer structure. Liu et al. [177] introduced highly sulfonated carbon nano-onions (CNOs) as excellent nanofillers into sulfonated PAES. They developed highly sulfonated CNOs by the thermal annealing method of nanodiamonds and underwent a sulfonation reaction with fuming H_2SO_4, illustrated in Fig. 13(a). The results indicate that the nanocomposite membrane exhibit excellent mechanical toughness enhanced water retention ability and good thermal and oxidative stability due to the good interfacial interfaces between the CNOs and SPAES. During the oxidative stability test using Fenton's reagent, the
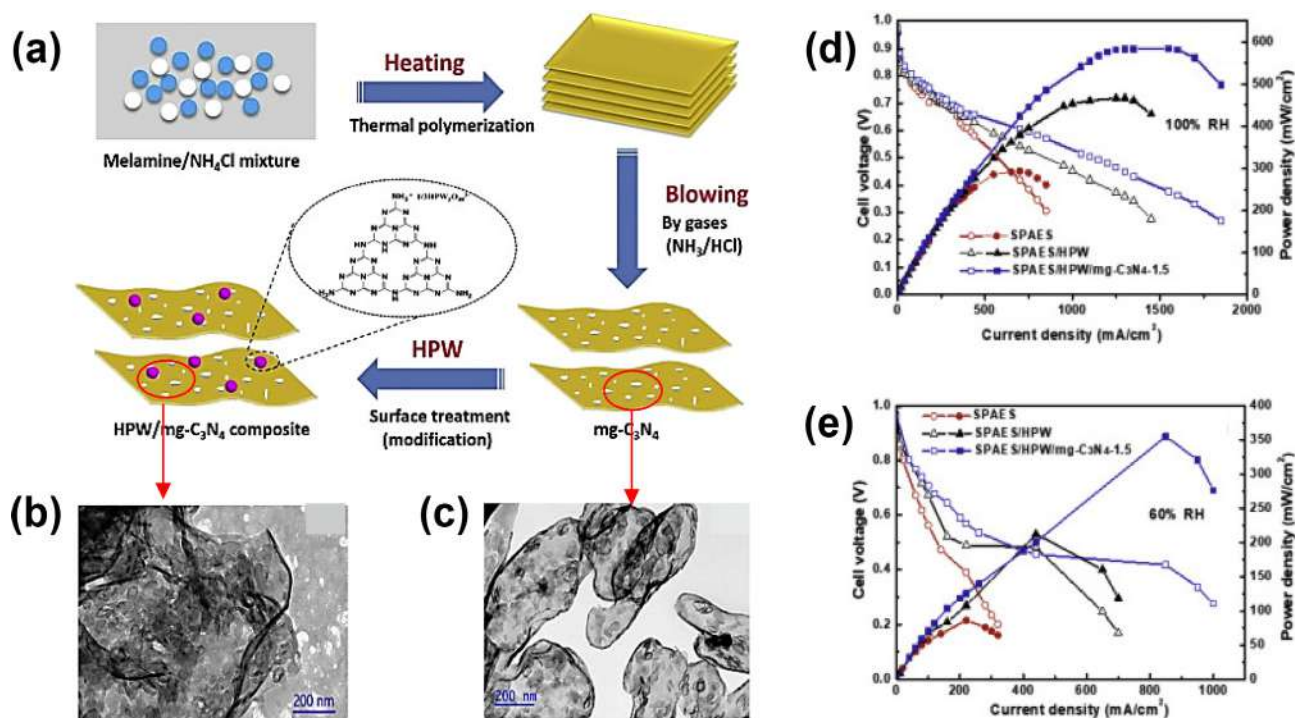
Fig. 14. (a) Synthetic diagram of the method to prepare HPW-mesoporous g-C$_3$N$_4$ nanofillers, (b) TEM images of mesoporous g-C$_3$N$_4$, (c) TEM images of HPW-mesoporous g-C$_3$N$_4$, (d) and (e) the polarization curve of the nanocomposite membrane testing at 100 % and 60 % RH conditions, respectively. Reprinted with permission from Ref.[182]. Copyright (2020) Elsevier.

nanocomposite membrane keeps its integrity longer than the pristine membrane, which results in excellent proton conductivity and mechanical durability. The hydroxyl attack of the hydrophilic segments of the polymer chain that leading loss of protonic site and mechanical deterioration. The obtained CNOs possess a uniform size of 5 nm with excellent interfacial interaction with SPAES that results in superior water retention properties that provide a better proton conductivity up to 0.18 S cm^{-1}, which is 45 % higher than pristine SPAES membrane (See Fig. 13(**b and c**)). Furthermore, the SPAES with highly sulfonated also shows better power density in H$_2$/O$_2$ cell performance as well as stability in cell voltage recorded over 168 h which it is comparable to Nafion® 112 membrane that is shown in Fig. 13(**d and e**).

Recently, graphitic carbon nitride (g-C$_3$N$_4$) has attracted attention as an emerging class of carbon materials due to its appropriate physicochemical properties that are highly demanded in various applications. Inexpensive, non-toxicity and simple preparation make this material widely explored as a filler for the composite membrane development [178]. Ingabire *et al.* [179] introduced different content of g-C$_3$N$_4$ nanosheet fillers incorporated into quaternized PAES (QPAES) membranes for AEMFC applications. The hydroxide conductivity was improved from 34.3 mS cm^{-1} to 46.5 mS cm^{-1} with 0.6wt% of g-C$_3$N$_4$ nanosheets tested at 80 °C. This research group also extended the application of g-C$_3$N$_4$ nanosheet filler by composite with TiO$_2$ nanoparticles to further enhance the hydroxide conductivity of the QPAES in AEMFC applications. This shows significant improvements in conductivity compared to previous reported AEM using these TiO$_2$/g-C$_3$N$_4$ fillers [180]. They also extended their research on these fillers incorporated into the SPAES in the PEMFC applications [181]. In this research, the composite TiO$_2$/g-C$_3$N$_4$ fillers show a grateful impact on the mechanical and dimensional stability of the SPPSU membrane, which is promising for long-term fuel cell operation. Besides that, Liu *et al.* [182] reported on the mesoporous g-C$_3$N$_4$ immobilized with phosphotungstic acid (HPW) as a filler to improve SPAES properties

as PEM in fuel cell applications. The surface of mesoporous g-C$_3$N$_4$ was modified with HPW (**see** Fig. 14(**a**)) to increase the active site for proton transportation. The TEM images in Fig. 14(**b and c**) show that the doped HPW hardly affected the structure of mesoporous g-C$_3$N$_4$. The fuel cell performance in this study shows that incorporating g-C$_3$N$_4$ into the SPAES membrane has shown a remarkable potential of g-C$_3$N$_4$ as a medium to improve the cell performance at high and low humidity conditions, as depicted in Fig. 14(**d and e**).

Silica

Silica-based nanoparticles have been extensively studied because of their low cost, inferior electrical conductivity, and better water retention capacity. Silica is commonly found in the crystalline state and rarely found in an amorphous state. Being a raw material in the glass and ceramic industries, silica has revolved around the development of the plastics industry. The hydrophilic nature of silica helps improve the proton conductivity of nanocomposite membranes. Wang *et al.* [183] modified the silica surface using nanoscale phosphonic acid as a filler in the Nafion membrane. The phosphonic acid functionalised silica fillers are well incorporated in the Nafion membrane and exhibited 24 % higher proton conductivity values than the unmodified Nafion membrane. This result agrees with a study reported by Oh *et al.* [184] that mentioned sulfonated silica nanocomposite membrane shows 2.8 times higher maximum power density compared to recast Nafion at 80 °C under low RH% conditions (20 %). Besides, Baglio *et al.* [185] studied the electrochemical behavior of sulfonated polysulfone composed of acidic silica nanoparticles for DMFC applications. This nanocomposite membrane resulted in a low swelling degree and lower methanol crossover. The particle size and structure of the fillers could affect the nanocomposite membrane properties. It was reported that the nanocomposite membranes with 30 nm particle size of nanofillers displayed 35 % higher proton conductiv-
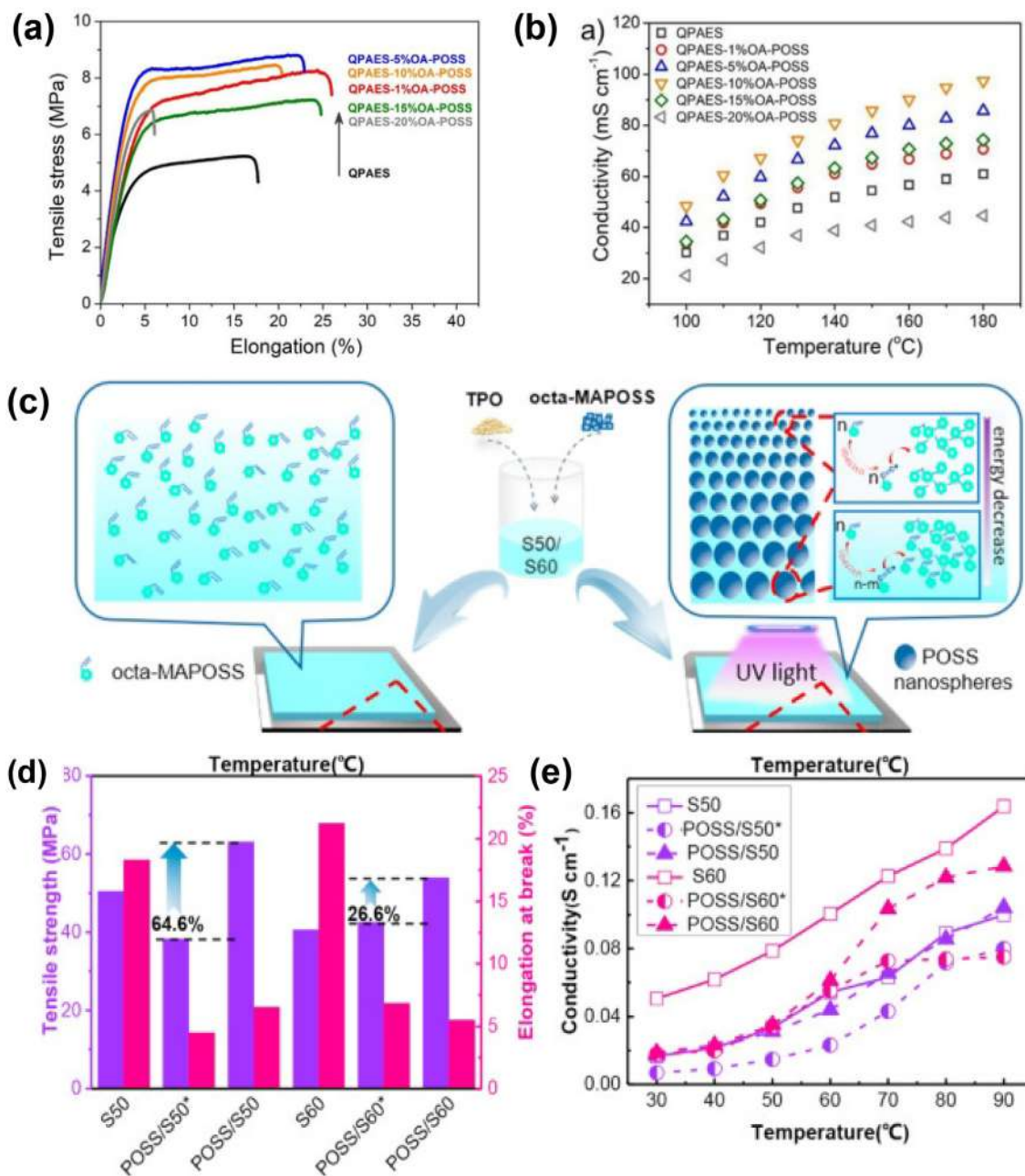
Fig. 15. (a) Tensile strength of the QPAES/OA-POSS nanocomposite membranes at 110 °C and (b) proton conductivity at different temperature. Reprinted with permission from Ref. [191]. Copyright (2021) Elsevier, (c) schematic illustration of POSS/SPAES with and without underwent UV radiation process, (d) mechanical properties and (e) proton conductivity of the POSS/SPAES nanocomposite membranes. Reprinted with permission from Ref. [192]. Copyright (2021) Elsevier.

ity than the nanocomposite membrane with micron-size particles [186]. Kim *et al.* [187] developed the nanocomposite membrane based SPAES polymer by incorporating various contents of mesoporous ceria-silica powder to test the durability of the nanocomposite membrane in PEMFC cells. The incorporation of mesoporous ceria-silica has indeed lowered the proton conductivity, but it has greatly enhanced the polymer degradation under oxidative stability test where cerium acts as a radical scavenger inside polymer matrices. They are testing the chemical durability of the nanocomposite membrane using H_2O_2 exposure in water vapor that is similar to actual conditions for PEMFC. The low weight loss percentage indicates that the nanocomposite membrane exhibits excellent chemical durability where cerium can act positively as a radical scavenger inside the SPAES polymer com-

posite membrane. Meanwhile, Ko *et al.* [188] introduced the core–shell silica particles into the SPAES polymer matrix. The SPAES bearing core–shell silica particle improves the dimensional stability, mechanical strength, and proton conductivity. The core–shell silica has shown well-connected hydrophilic channels with the SPAES polymer chains, greatly enhancing the SPAES membrane properties.

In comprehensive materials technologies, silicon-containing organic polymers, silsesquioxane have generated tremendous interest because of their potential replacement and compatibility with silicon-based inorganics. Silsesquioxane is a silicon-oxygen cage compound of the general formula $(RSiO_{0.5})n$ in which R can be any kind of organic group and H except O group [189]. Silsesquioxane cage-like structure is usually called polyhedral

oligosilsesquioxanes or polyhedral oligomeric silsesquioxane, abbreviated as POSS. Conceptually, it can be considered the smallest possible silica particle with a diameter range of 1–3 nm, which has been created either with a dispersant or coupling agent depending upon the type [190]. POSS nanoparticles have recently been widely explored in the polymer matrix-based proton exchange membrane as a filler. Wang et al. [191] introduced octa amino POSS (OA-POSS) fillers into quaternary ammonium PAES molecular structure to determine the effect on the mechanical properties and proton conductivity values of the PEM. The interaction between hydrophilic OA-POSS shows a high proton conductivity of 97.4 % mS cm^{-1} at 180 °C without humidification, and the tensile stress acquired about 70 % higher as compared to pristine quaternary ammonium PAES testing at 110 °C (see Fig. 15(a and b)). It indicates that the hydrophilic OA-POSS are excellently compatible with the quaternary ammonium PAES by the reactions with the amino groups, which exhibit excellent PEM properties operated at higher cell temperatures.

POSS nanoparticles containing octahedral structures with the external organic functional group can be easily modified to be compatible with various polymer matrices, even at very low concentrations [193]. Nor et al. [194] reported the study on the effect of modified POSS by sulfonation incorporated into highly sulfonated PPSU polymers. It shows that the POSS was successfully modified by adding eight sulfonic acid groups on the outer surface of the POSS and the compatibility with SPPSU was excellent. They further investigated the effect of the SPOSS loading, and it shows that SPOSS greatly enhanced the membrane flexibility and proton conductivity [195]. Integrating organic–inorganic POSS nanoclusters into a polymer matrix would contribute in enhancing the nanocomposite membrane properties, such as controlling the membrane swelling while maintaining the proton conductivity of the sulfonated polymers[20,196]. Chen et al. [192] introduced gradient-distributed POSS nanospheres dispersed in sulfonated PAES via UV radiation. Fig. 15(c) shows the schematic illustration of POSS nanospheres in the SPAES membrane without (POSS/S*) and with underwent the UV (POSS/S) induced polymerization process. In Fig. 15(d), the SPAES/POSS underwent a UV radiation process showing high mechanical strength and enhanced membrane flexibility. On the other hand, the UV radiation process enhances the interfacial interaction of SPAES with POSS, where the proton conductivity was significantly higher at a higher temperature, as shown in Fig. 15(e). Most POSS nanoclusters can be incorporated into most existing polymers through blending, grafting, or copolymerization, resulting in significant improvements to several polymer properties. The properties of SPAES/polydopamine-modified sulfonated POSS were reported by Zhang et al. [83] to address the trade-off between membrane stability and proton conductivity values for PEMFC. They concluded that the interaction between the sulfonate group of POSS or SPAES with primary groups of polydopamine could maintain the superior mechanical strength of the nanocomposite membrane with an excellent proton hopping site that results in high proton conductivity. The oxidative stability of the polydopamine-modified sulfonated POSS effectively protect the polymer backbone from radical attacks where higher IEC membrane leads to the volumetric suspension that allow more radicals attacks that reducing the chemical durability. Notably, incorporating modified POSS fillers can enhance the proton conductivity, mechanical strength, and single-cell performance of the PEM.

Inorganic clay

Polymer-inorganic nanocomposite materials herein are defined as inorganic nanofillers dispersed at a nanometer level in a polymer matrix to enhance the polymer matrix properties. It may combine the advantages of the inorganic materials and the polymer matrix itself. The organic–inorganic nanocomposite materials have developed rapidly due to the excellent application prospects in both structures and functions [197]. Among the inorganic materials widely being explored as a filler in the polymer electrolyte membrane, clay is one of them. Clay or layered silicate is a fine-grained natural rock or soil material that combines several clay minerals with possible traces of quartz, metal oxides, and organic matter [198]. Different types of clay and their various physical and chemical properties are determined by their chemical composition and structure [199]. Clay works very well as electrolytes, especially as a filler in the nanocomposite membrane for fuel cells, depending on its structure, morphology, size, and ionic nature [200]. A study by Plackett et al. [201] reports that incorporating modified laponite clay in polybenzimidazole membrane for high-temperature fuel cell applications and the nanocomposite membrane shows good mechanical strength as well as improve in dimensional stability. Other than that, Neethu et al.[199] developed a nanocomposite membrane using natural clay incorporated into activated carbon from coconut shells for a microbial fuel cell. This nanocomposite membrane exhibited excellent properties as a membrane fuel cell.

Montmorillonite, hectorite, and saponite are the most used layered silicate. Montmorillonite (MMT) has been a filler of choice for most studies on polymer nanocomposite due to its high cation exchange capacity, high surface areas, high surface reactivity, and high barrier properties [202]. The general formula of MMT is M_x $(AL_{4-x}Mg_x)Si_8O_{20}(OH)_4$. This MMT nanomaterial consists of a 1 nm thick aluminosilicate layer stack with a regular gap. Despite the advantages of MMT clay, the chemical microstructure behaviour has limited the usage of MMT as a filler. Using different modifiers, modifying the MMT surface could prevent the phase inconsistency between organic polymer membrane and inorganic clay. Nafion composite membrane with the presence of sulfonated MMT shows significantly reduced methanol permeability for DMFC applications. At the same time, the proton conductivity also reduces a bit compared to the pristine Nafion membrane [203].

Other than that, porous aluminosilicate materials are attractive due to their textural and surface features, highly ordered structures, high surface area, and wide pore-range/pore size distribution. The porous morphology of aluminosilicate facilitates specific ionic interactions with the host matrix and enhances water uptake and other related properties of the nanocomposite membrane. Imogolite is a class of inorganic clay that contains aluminium silicate clay mineral that is in a nanotubular structure with unique physicochemical properties [204]. The nanotubular imogolite has a large surface area of up to micrometers comprised of aluminium hydroxide on the outer wall and a silicate layer in the inner wall [205]. Nor et al. [29] introduced various loading of imogolite nanotube to improve the properties of the crosslink highly sulfonated PPSU for PEMFC. The imogolite consists of the alumina and silica elements depicted in the FTIR figure and the chemical structure illustrated in Fig. 16(a). Incorporating 1 wt% of imogolite loading has significantly improved the membrane water uptake, contributing to cell performance improvements from 77.2 mW cm^{-2} to 111.2 mW cm^{-2} tested at 80 °C and 100 % RH (see Fig. 16(d)). The flexibilities of the membrane were also enhanced as a remark on an excellent interface in MEA preparation (see Fig. 16(b)). The nanocomposite membrane also shows superior chemical stability in the Fenton test as the membrane remains intact over the period of testing time shown in Fig. 16(c). Like CNT, imogolite has a high aspect ratio, and surface area with tube length runs from several hundred nanometers to micrometres. However, some imogolite nanotechnology problems remain to be overcome, for instance, the uniform dispersion inside a polymer matrix, tenability of imogolite dimensions (diameter and length), and interfacial adhesion between the nanotube and the polymer matrix [206].
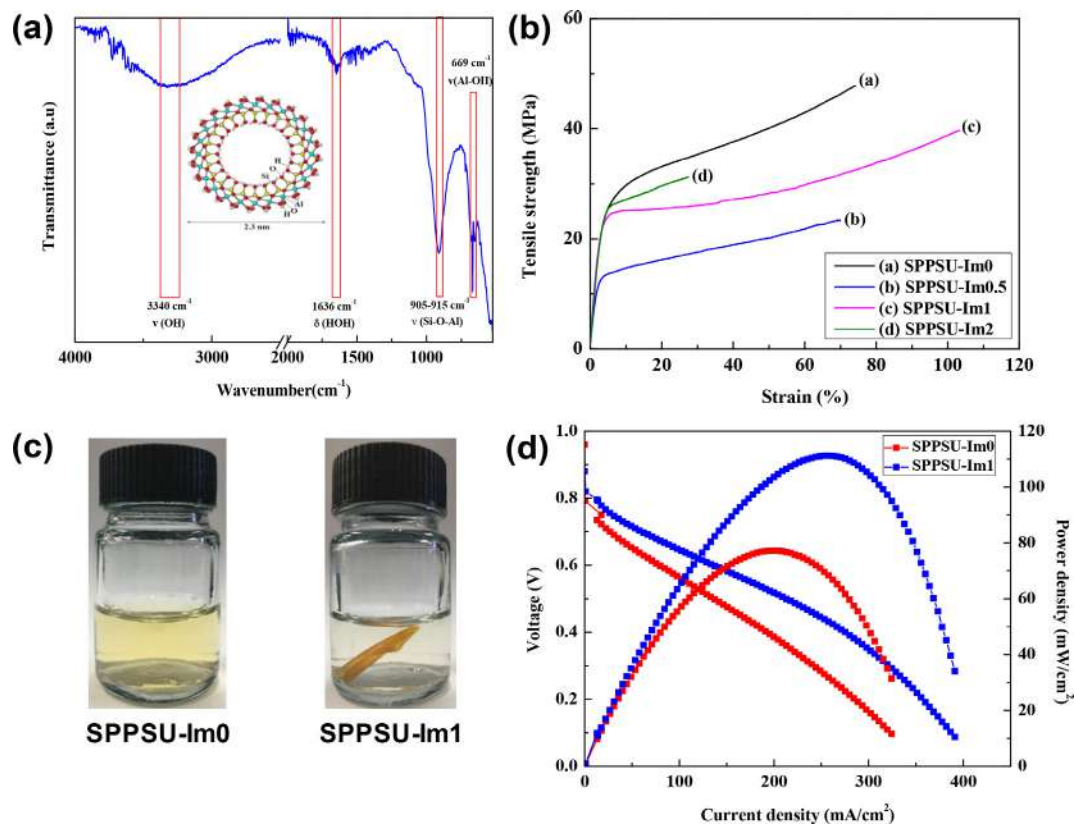
Fig. 16. (a) FTIR spectra and chemical structure of the imogolite, (b) the stress–strain curve of the nanocomposite membrane, (c) the membrane condition after immersing in the Fenton reagent for 14 days and (d) the I-V polarization curve of SPPSU and SPPSU-imogolite nanocomposite membrane tested at 80 °C, 90 % RH. Reprinted with permission from Ref. [29]. Copyright (2021) Elsevier.

Although there are not many reports on the application of imogolite as a filler in the polymer electrolyte membrane, it is still worth studying this material as a filler with the advantages mentioned above on these materials.

Metal oxide

The former inorganic component in the polymeric material can enhance membranes' mechanical strength and stability of membranes while suppressing fuel diffusion and swelling of membranes. The latter can combine the appealing advantages of each component and reduce their weaknesses. On the other hand, it has been demonstrated that adding metal oxide into a polymer matrix could improve the mechanical properties of polymer electrolyte membranes [34,207]. Metal oxide refers to crystalline solids that contain a metal cation and an oxide anion. They typically react with water to form bases or acids to form salts. Usually, metal oxides such as TiO_2, SiO_2, or ZrO_2 can be classified as hygroscopic materials in which these materials can attract and hold water molecules via either absorption or adsorption from the surrounding. The purpose of having hygroscopic metal oxides as a filler is to enhance the water retention capacity of the nanocomposite for better proton transportation. Li *et al.* [208] reported on the Nafion nanocomposite membrane consisting of SiO_2 and ZrO_2 by in situ hydrolysis through the sol–gel process. These metal oxide nanoparticles have fair distribution in the Nafion membrane with diameters of ∼5 nm and adequate water retention capacity, contributing to good proton conductivity values at all measured temperature ranges. Li *et al.* [209] reported incorporating different wt% nano-ZrO_2 particles into the multi-block copolymer of PPSU for AEMFC. The incorporation of nano-ZrO_2 particles significantly

improved the membrane water uptake, ionic conductivity, alkaline stability, and mechanical properties. Liu *et al.* [210] study on the superacid sulfated SnO_2 doped with CeO_2 (CST) as a novel inorganic filler for SPAES-based PEM. This study highlights the effect of the incorporation of novel dual metal oxide on the proton conductivity of the nanocomposite membrane in fuel cell applications (see Fig. 17(**a and b**)). The better compatibility of the CST nanoparticles with SPAES molecular structure was observed on the SEM images, where the SEM images showed a smoother surface as compared to SPAES with sulfated SnO_2 (ST) particles (see Fig. 17(**c–e**)). This novel inorganic filler has provided an excess active site for proton conduction that can help improve the proton conductivity of the nanocomposite membrane. The superacid metal oxide fillers also have taken part in enhancing the durability of the SPPSU membrane under accelerated stress test conditions that contribute to comparable cell performance with the commercial Nafion 112 membrane (see Fig. 17(**f and g**)). The oxidative test in Fenton's reagent shows high chemical resistance of the nanocomposite membrane that also results in stable cell voltage under prolonged operating time.

Titanium dioxide or titania is a type of metal oxide that is thermally stable, poorly soluble, highly resistant to corrosion, and classified as not hazardous material [211]. Titania has become one of the remarkable inorganic materials that the researcher has been focusing on due to its unique properties, environmental friendliness, and most important property that it is economical. Titania provides many benefits in enhancing fuel cell performance as electrolytes or electrodes [212,213]. The titania crystal structure in anatase or rutile is thermodynamically stable, contributing to the composite materials' good thermal and chemical stability. Titania with high surface area in the nanocomposite membranes shows
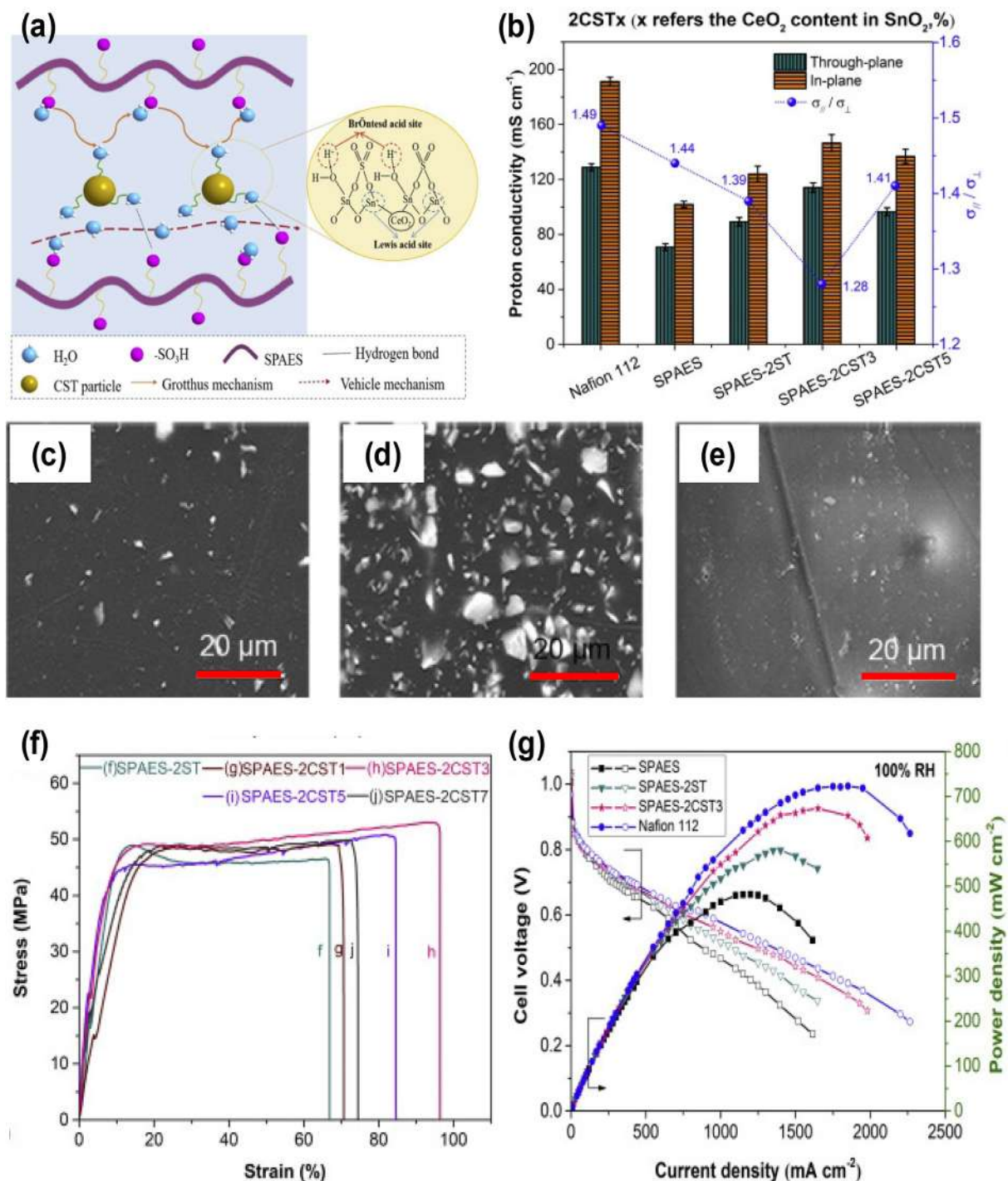
Fig. 17. (a) The possible proton conduction mechanism in nanocomposite membrane, (b) In-plane conductivity of the nanocomposite membrane compared with pristine SPPSU and Nafion 112 membrane measured at 90 °C in water, SEM images on SPAES with (c) 2 wt% ST, (d) 5 wt% ST, (e) 2wt% CS + 3 wt% ST, (f) stress–strain curve and (d) single cell test performance of the sample membrane compared with Nafion 112 tested at 80 °C and 100 % RH. Reprinted with permission from Ref. [210]. Copyright (2021) Elsevier.

good thermal stability and improves water uptake, enhancing membrane conductivity. Furthermore, titania with a higher active surface area can also increase the active area for reaction, preventing sintering and limiting the electrocatalyst's poisoning [214]. Devrim et al. [215] reported that the nanocomposite-based proton exchange membrane consists of the sulfonated polysulfone membrane incorporating titanium dioxide nanoparticles. It shows that TiO_2 increased the thermal stability of the membrane but upon higher loading, causing a brittle membrane due to the agglomera-

tion of the TiO_2 nanoparticles. Zhang et al. [216] reported using modified TiO_2 using sulfonation to enhance the dispersion of these nanoparticles into the SPAES microstructure. From the findings, incorporating the sulfonated titania ($STiO_2$) has improved the membrane water uptake and reduced membrane swelling, which are important factors in maintaining membrane stability. Better dispersion of sulfonated titania was observed in Fig. 18(a–f), where no white particle was observed on the membrane surface when the sulfonated titania was used.
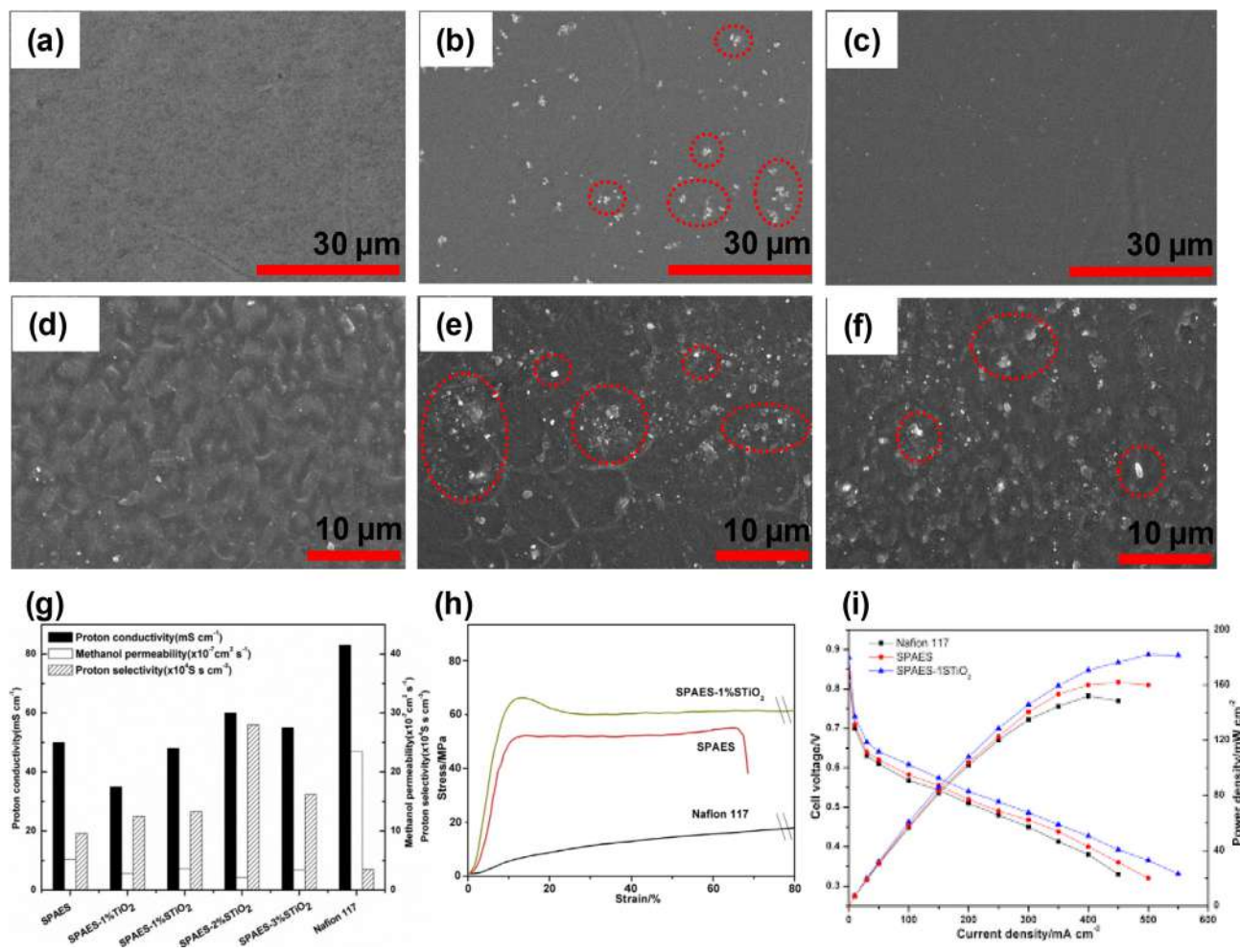
Fig. 18. The SEM images of nanocomposite membrane on surface (a-c) and cross sectional images (d-f) where (a, d) SPAES membrane, (b, e) SPAES-1 % TiO$_2$, (c,f) SPAES-1 % STiO$_2$, (g) proton conductivity, methanol permeability and proton selectivity of the sample membrane at 30 °C, (h) mechanical properties of SPAES, SPAES-1 % STiO$_2$ and Nafion 117 membranes, and (i) DMFC performance of SPPSU, SPPSU-1 %STiO$_2$ and Nafione membrane at 80 °C. Reprinted with permission from Ref. [216]. Copyright (2020) John Wiley and Sons.

In contrast, less white particle was observed on the cross-sectional images. The incorporation of the titania nanoparticles also shows an exceptional improvement towards reducing the methanol permeability of the cell, and improvement in membrane flexibilities was shown in Fig. 18**(g and h),** which contributes to better DMFC performance as compared to pristine SPPSU membrane and commercial Nafion117 membrane (see Fig. 18**(i)**). In every modification of PPSU-based PEM membrane, incorporating different type of additives such as carbonaceous materials, silica, inorganic clay, and metal oxide that have been discussed give improvements towards physicochemical membrane properties in many ways. The significant improvements are towards the mechanical and stability of the nanocomposite membranes under appropriate amounts of additives. Proper optimizations of the additives quantity that are integrated into the PPSU membrane matrix will result in excellent membrane properties that will give efficient fuel cell performance. The various nanocomposite membrane based PPSU in fuel cell application is summarized in Table 4**.**

Future outlooks of SPPSU membrane modification for PEMFC

Fuel cell technology is two to three times more efficient than fuel burning. No other energy generation technology offers the benefits that fuel cell technology can offer. In addition to low or zero emissions, benefits include high efficiency and reliability, multi-fuel capability, flexibility, durability, scalability, and ease of maintenance. It has attracted scientists and industries to research this technology since it has had a considerable impact on the R&D industries. Research has been explored to improve the properties of every part of the fuel cell system, and the electrolyte membrane has a significant impact on cell performance. The important function of PEM in the fuel cell system has initiated many studies to develop PEM with high proton conductivity and good mechanical, thermal, and oxidative stability. These properties should remain unchanged at the working temperature to avoid structural change during the chemical reactions. Proton-conducting polymer electrolyte based on highly sulfonated PPSU polymers is one of the promising materials for developing new PEMFCs as a replacement to the expensive Nafion membrane. These polymer materials have a great variety concerning the chemical structure and can be chemically modified for better properties as a proton exchange membrane. PPSU have a very great structure that can withstand very harsh acidic conditions during the sulfonation process for a period of time. The innovation of implementing thermal crosslinking steps to counter the problems of having a weak mechanical character of highly sulfonated polymers becomes fascinating research worth exploring.

Table 4

Nanocomposite based PPSU membrane in fuel cell applications.

Composite membrane	Conductivity (S cm^{-1})	Mechanical strength (MPa)	Elongation at break (%)	Water uptake/ swelling RT (%)	Power density (mW cm^{-2})	Temperature (°C)	RH (%)	Type of fuel cell
SPAES/polydopamine modified SPOSS[83]	0.243, 80 °C, 100 % RH	50.82	7.25	40/14	346	70	100	PEMFC
SPPSU/CND[28]	0.0364, 80 °C, 90 % RH	55.5	121.5	82/20	118.75	80	100	PEMFC
SPAES/poly(2,5-benzimidazole)-grafted GO[170]	0.153, 80 °C, 90 % RH	59.47	43.78	-	-	-	-	PEMFC
SPAES grafted GO[171]	0.146, 90 °C, 90 % RH	55.5	9.5	75.9/63.2	-	-	-	PEMFC
SPAES/SATS-GO[172]	0.131, 80 °C, 90 % RH	62.2 ± 3.0	36.8 ± 3.7	-	-	-	-	PEMFC
SPAES/perfluoropolyether-functionalized GO[174]	~0.200, 80 °C, 90 % RH	72.4 ± 4.6	18.2 ± 4.2	55.4/21.7	-	-	-	PEMFC
SPAES/polytriazole grafted GO[173]	0.413, 80 °C, 90 % RH	53.8 ± 2.6	12.2 ± 0.8	58/75	1580	80	100	PEMFC
QPAES/g-C3N4[179]	0.0465, 80 °C, 100 % RH	25.8 ± 1.0	31.0 ± 2.8	-	68.1	60	100	AEMFC
Q-PAES-TiO2/g-C3N4[180]	0.0438, 80 °C, 100 % RH	26.2	16.4	70.2/21.7	64.3	60	100	AEMFC
SPAES-TiO$_2$/g-C$_3$N$_4$[181]	0.325, 80 °C, 100 % RH	34.8	132.9	63.5/19.2	273.9	80	100	PEMFC
SPAES/phosphotungstic acid-gC$_3$N$_4$[182]	0.203, 80 °C, 100 % RH	43.2	~54	37.1/0.7	584	80	100	PEMFC
SPAES/core–shell poly(4-vinylpyridine) silica nanoparticles[188]	16.01 kJ/mol, 80 °C, 90 % RH	72.45	11.14	34.29/37.39	-	-	-	PEMFC
PAES/octa-amino POSS[191]	0.097, 180 °C, – % RH	8.5	21	48.6/0.95	429	180	-	HT-PEMFC
SPAES/POSS nanospheres[192]	0.09, 80 °C, 100 % RH	~65	~7	/5.9	-	-	-	PEMFC
SPPSU/Imogolite[29]	0.0436, 80 °C, 90 % RH	39.7	103.3	30/23.5	111.2	80	90	PEMFC
Multiblock QPAES/nano-ZrO$_2$[209]	0.0552, 80 °C, 100 % RH	32.0 ± 2.6	27.2 ± 2.2	56.2/15.4	-	-	-	AEMFC
SPAES/SnO$_2$-CeO$_2$[210]	0.128, 80 °C, 100 % RH	52.9	96	43.9/5.9	673.6	80	100	PEMFC
SPAES/S-TiO$_2$[216]	0.048, RT °C, 100 % RH	65.7	171	37/9	~180	80	-	DMFC
Elctrospun PSf/spray SPAES[217]	0.0763, -°C, -% RH	~35	~80	-/10.25	611.2	80	100	PEMFC
Sulfonated fluorinated block copolymers SPPSU-functionalized silica[218]	0.100, 90 °C, 100 % RH	41.5	2.7	72.1/-	-	-	-	PEMFC
4-amino phenyl pendants SPPSU/ SiO$_2$-SO$_3$H[219]	0.110, 100 °C, 100 % RH	28	25.5	35/-	-	-	-	DMFC
SPPSU/phosphotungstic acid/silica[220]	0.151, 80 °C, 100 % RH	19	24	38.6/-	450	85	100	PEMFC

In addition, the modification of the SPPSU membrane toward membrane stability and durability in fuel cell applications by implementing different types and structures of inorganic fillers with unique properties are fascinating subjects to be discovered. As mentioned above, several modifications have been made with the incorporation of different types and structures of fillers, has been reported to improve the properties of the SPPSU as a PEM in a fuel cell system. Different types and structures of inorganic fillers incorporated into SPPSU polymers have improved the SPPSU membrane properties essential for PEMFC applications. The research presented the key factors that influence the SPPSU nanocomposite membrane consisting of the different types and structures of fillers to serve as a basis in the rational design of a new PEM in fuel cell applications. Implementing the fillers into the SPPSU matrix should be extensively studied to reduce the trade-off between the attractive fillers and polymer properties. Besides, new emerging fillers with surface modifications such as nitrogen-doped, acid-doped, and base-doped that have superior compatibilities with polymer-based membranes have gained much attention from researchers and industry. Since that, the acid-doped filler can also improve the water properties of the membrane and provide an additional proton conduction medium for enhancing the proton conductivity values. It would be successful in the com-

mercialization of the fuel cell system with the implementation of natural-based based fillers inside the SPPSU polymer matrix since it will lower the cost of materials and membrane process. The nanocomposite polymer membrane can be identified as a remarkable family of the proton-conducting membrane, which provides new high performance that can be operated under any conditions and be commercialized.

Conclusions

Implementing different fillers into the polymer-based membrane involves a variety of technologies that the fillers have contributed substantially to the material engineering field. This study focuses on the different types and structures of fillers incorporated into the sulfonated PPSU polymer membrane to replace the commercial Nafion membrane to reduce the membrane processing cost and any major problems facing the Nafion membrane. This review briefly discussed the role of different types of nanocomposite membrane bearing SPPSU as a polymer backbone, such as multi-block copolymers, carbonaceous nanomaterials, silica, inorganic clay, and metal oxide for fuel cells. Fillers with nanoscale particle size ranges are favourable as filler as smaller molecular size enables easier dispersion in narrow hydrophilic

nanochannels and may enlarge the nanochannel size for better proton transportation. Besides that, the incorporation of inorganic fillers has effectively suppressed excessive water absorption and increased the tensile strength of the nanocomposite membrane. The surface modification of the fillers into the SPPSU membrane has provided an external proton source for higher proton conductivity and improved the compatibility with a different matrix. It is interesting to state that the utilization of a variety of fillers show excellent membrane and electrochemical properties. Besides that, this study also discusses the possibility of implementing thermal crosslinking to improve the poor mechanical and dimensional stability of the highly sulfonated PPSU without sacrificing the proton conductivity values. Given the satisfactory proton conductivity, good dimensional, mechanical properties, and chemical durability, and different types of fillers under normal fuel cell operating conditions, the developed nanocomposite membranes are good enough to compete with commercial PEM in the market.

Declaration of Competing Interest

Acknowledgements

References

[1] H. Ritchie, M. Roser, OurWorldInData.org., https://ourworldindata.org/ozone-layer, 2018 (accessed on 9 October 2021).
[2] D. Gielen, F. Boshell, D. Saygin, M.D. Bazilian, N. Wagner, Energy, Strateg. Rev. 24 (2019) 38–50, https://doi.org/10.1016/j.esr.2019.01.006.
[3] A. Kalair, N. Abas, M.S. Saleem, A.R. Kalair, N. Khan, Energy, Storage 3 (2021), https://doi.org/10.1002/est2.135.
[4] S.S. Siwal, S. Thakur, Q.B. Zhang, V.K. Thakur, Mater. Today Chem. 14 (2019), https://doi.org/10.1016/j.mtchem.2019.06.004.
[5] A. Triandafyllidou, M. McAuliffe, Report Overview, Migr, Smuggling Data Res. (2019) (accessed on 30 December 2021).
[6] M.S. Ahmad, M.S. Ali, N.A. Rahim, Energy, Strateg. Rev. 35 (2021), https://doi.org/10.1016/j.esr.2021.100632.
[7] M.M. Tellez-Cruz, J. Escorihuela, O. Solorza-Feria, V. Compañ, Polymers 13 (2021) 1–54, https://doi.org/10.3390/polym13183064.
[8] V.A. Sethuraman, A.Z. Weber, J.W. Weidner, Encycl. Electrochem. Power Sources, Elsevier B. (2009) 817–827.
[9] C. Sealy, Mater. Today 11 (2008) 65–68, https://doi.org/10.1016/S1369-7021(08)70254-2.
[10] Y. Manoharan, S.E. Hosseini, B. Butler, H. Alzhahrani, B.T.F. Senior, T. Ashuri, J. Krohn, Appl. Sci. 9 (2019) 2296, https://doi.org/10.3390/app9112296.
[11] P. Tölle, C. Köhler, R. Marschall, M. Sharifi, M. Wark, T. Frauenheim, Chem. Soc. Rev. 41 (2012) 5143–5159, https://doi.org/10.1039/c2cs15322j.
[12] P.J. Hamilton, B.G. Pollet, Fuel Cells 10 (2010) 489–509, https://doi.org/10.1002/fuce.201000033.
[13] X. Sun, S.C. Simonsen, T. Norby, A. Chatzitakis, Membranes 9 (2019) 9070083, https://doi.org/10.3390/membranes9070083.
[14] E. Bakangura, L. Wu, L. Ge, Z. Yang, T. Xu, Prog. Polym. Sci. 57 (2016) 103–152, https://doi.org/10.1016/j.progpolymsci.2015.11.004.
[15] N. Shaari, S.K. Kamarudin, Energy, Res. 43 (2019) 2756–2794, https://doi.org/10.1002/er.4348.
[16] P. E. Dodds, A. Staffel, A. D. Hawkes, F. Li, P. Grunewald, W. McDowall, P. Ekins, Int. J. Hydrogen Energy 40(2015) 2065-2083. 10.1016/j.ijhydene.2014.11.059.

[17] C. Meemuk, S. Chirachanchai, Int. J. Hydrogen Energy 43(2018) 6701-6710. 10.1016/j.ijhydene.2018.02.092.
[18] N.A.M. Harun, N. Shaari, N.F.H. Nik Zaiman, Int. J. Energy Res. 45(2021) 19671-19708. 10.1002/er.7048.
[19] A.S. Abdulkareem, A.S. Afolabi, C.A. Idibie, S.E. Iyuke, H.C.v.Z. Pienaar, Energy Procedia 14 (2012) 2026-2037. 10.1016/j.egypro.2011.12.1204.
[20] J. Zhang, F. Chen, X. Ma, X. Guan, D. Chen, M.A. Hickner, Int. J. Hydrogen Energy 40(2015) 7135-7143. 10.1016/j.ijhydene.2015.02.090.
[21] H. Pan, Y. Zhang, H. Pu, Z. Chang, J. Power Sources 263 (2014) 195–202, https://doi.org/10.1016/j.jpowsour.2014.04.055.
[22] S. Rogalsky, J.–F. Bardeau, S. Makhno, O. Tarasyuk, N. Babkina, T. Cherniavska, M. Filonenko, K. Fatyeyeva, Mater. Today Chem. 20(2021) 100453. 10.1016/j.mtchem.2021.100453.
[23] B. Motealleh, F. Huang, T.D. Largier, W. Khan, C.J. Cornelius, Polymer 160 (2019) 148–161, https://doi.org/10.1016/j.polymer.2018.11.045.
[24] Harilal, R. Nayak, P.C. Ghosh, T. Jana, ACS Appl. Polym. Mater. 2(2020) 3161-3170. 10.1021/acsapm.0c00350.
[25] P. Sun, Z. Xia, Z. Li, Z. Fan, F. He, Q. Liu, X. Yin, Mater. Today Chem. 23(2022) 100653. 10.1016/j.mtchem.2021.100653.
[26] N. Krathumkhet, K. Vongjitpimol, T. Chuesutham, S. Changkhamchom, K. Phasuksom, A. Sirivat, K. Wattanakul, Solid State Ionics 319(2018) 278-284. 10.1016/j.ssi.2018.02.019.
[27] L. Assumma, C. Iojoiu, G. Albayrak Ari, L. Cointeaux, J.Y. Sanchez, Int. J. Hydrogen Energy 39(2014) 2740-2750. 10.1016/j.ijhydene.2013.07.090.
[28] N.A. Mohamad Nor, H. Nakao, J. Jaafar, J.D. Kim, Int. J. Hydrogen Energy 45 (2020) 9979-9988. 10.1016/j.ijhydene.2020.01.142.
[29] N.A. Mohamad Nor, K. Tamura, J. Jaafar, J.D. Kim, A.F. Ismail, M.H.D. Othman, M.A Rahman, J. Environ. Chem. Eng. 9(2021) 105641. 10.1016/j.jece.2021.105641.
[30] J. Wang, C. Gong, S. Wen, H. Liu, C. Qin, C. Xiong, L. Dong, Int. J. Hydrogen Energy 44(2019) 6909-6918. 10.1016/j.ijhydene.2019.01.194.
[31] J.D. Kim, L.J. Ghil, Int. J. Hydrogen Energy 41(2016) 11794-11800. 10.1016/j.ijhydene.2016.02.084.
[32] J.W. Park, R. Wycisk, P.N. Pintauro, V. Yarlagadda, T. Van Nguyen, Materials 9 (2016) 9030143, https://doi.org/10.3390/ma9030143.
[33] H. Lade, V. Kumar, G. Arthanareeswaran, A. F. Ismail, Int. J. Hydrogen Energy 42(2017) 1063-1074. 10.1016/j.ijhydene.2016.10.038.
[34] L. Chen, S. Chai, K. Liu, N. Ning, J. Gao, Q. Liu, F. Chen, Q. Fu, A.C.S. Appl, Mater. Interfaces 4 (2012) 4398–4404, https://doi.org/10.1021/am3010576.
[35] K.B.N. Balasubramanian, T. Ramesh, Polym. Adv. Technol. 29 (2018) 1568–1585, https://doi.org/10.1002/pat.4280.
[36] W. Liu, B. Ullah, C.-C. Kuo, X. Cai, Adv. Polym. Technol. 2019 (2019) 4294306, https://doi.org/10.1155/2019/4294306.
[37] K. Kordesch, M. Cifrain, Handb, Fuel Cells-Fundamental, Technology and Applications Handb. Fuel Cells, John Wiley & Sons, Ltd. (2010), https://doi.org/10.1002/9780470974001.f304065.
[38] T. Dey, J. Deshpande, D. Singdeo, P.C. Ghosh, J. Energy 2019 (2019) 3821082, https://doi.org/10.1155/2019/3821082.
[39] R.K.S.S. Vuppala, B.A. Chedir, L. Jiang, L. Chen, M. Aziz, A.P. Sasmito, Molecules 24 (2019) 24173097, https://doi.org/10.3390/molecules24173097.
[40] D.R. Dekel, J. Power Sources 375 (2018) 158–169, https://doi.org/10.1016/j.jpowsour.2017.07.117.
[41] E. Ogungbemi, T. Wilberforce, O. Ijaodola, J. Thompson, A.G. Olabi, Int. J. Energy Res. 45 (2011) 1227–1245, https://doi.org/10.1002/er.5810.
[42] A.A. Abd El Monem, A.M. Azmy, S.A. Mahmoud, Ain Shams Eng. J. 5 (2014) 75–84, https://doi.org/10.1016/j.asej.2013.05.001.
[43] A. Syampurwadi, H. Onggo, Indriyanti, R. Yudianti, J. Phys. Conf. Ser. 755 (2016) 012029. 10.1088/1742-6596/755/1/011001.
[44] G.H. Guvelioglu, H.G. Stenger, J. Power Sources 147 (2005) 95–106, https://doi.org/10.1016/j.jpowsour.2005.01.011.
[45] S. Authayanun, W. Pothong, K. Ngamsai, A. Patniboon, A. Arpornwichanop, Energy Procedia 61 (2014) 1553–1556, https://doi.org/10.1016/j.egypro.2014.12.168.
[46] P.H. Lee, S.S. Hwang, Sensors 9 (2009) 9104–9121, https://doi.org/10.3390/s91109104.
[47] S. Yu, D. Jung, Renew. Energy 33 (2008) 2540–2548, https://doi.org/10.1016/j.renene.2008.02.015.
[48] Z. Belkhiri, M. Zeroual, H. Ben Moussa, B. Zitouni, Rev. des Energies Renouvelables 14(2011) 1-121. [Online]. Available: http://www.webreview.dz/IMG/pdf/Effect_of_temperature_and_water_content_on.pdf.
[49] M. Rahsepar, M. Pakshir, P. Nikolaev, Y. Piao, H. Kim, Int. J. Hydrogen Energy 39 (2014) 15706–15717, https://doi.org/10.1016/j.ijhydene.2014.07.152.
[50] O.T. Holton, J.W. Stevenson, @BULLETPlatinum Met, Rev 57 (2013) 259–271, https://doi.org/10.1595/147106713x671222.
[51] R. Espiritu, M. Mamlouk, K. Scott, Int. J. Hydrogen Energy 41 (2016) 1120–1133, https://doi.org/10.1016/j.ijhydene.2015.10.108.
[52] I.P. Sahu, G. Krishna, M. Biswas, M.K. Das, Energy Procedia 54 (2014) 468–478, https://doi.org/10.1016/j.egypro.2014.07.289.
[53] C. Yin, J. Li, Y. Zhou, H. Zhang, P. Fang, C. He, A.C.S. Appl, Mater. Interfaces 10 (2018) 14026–14035, https://doi.org/10.1021/acsami.8b01513.
[54] P. Lin, P. Zhou, C.W. Wu, J. Power Sources 194 (2009) 381–390, https://doi.org/10.1016/j.jpowsour.2009.04.068.
[55] P. Thounthong, B. Davat, S. Raël, IEEE Power Energy Mag. 6 (2008) 69–76, https://doi.org/10.1109/MPAE.2008.4412942.
[56] S. Banerjee, D.E. Curtin, J. Fluor. Chem. 125 (2004) 1211–1216, https://doi.org/10.1016/j.jfluchem.2004.05.018.

[57] G.G. Gagliardi, A. Ibrahim, D. Borello, A. El-Kharouf, Molecules 25 (2020) 25071712, https://doi.org/10.3390/molecules25071712.

[58] S.G.A. Flimban, S.H.A. Hassan, M.M. Rahman, S.E. Oh, Int. J. Hydrogen Energy 45 (2020) 13643–13651, https://doi.org/10.1016/j.ijhydene.2018.02.097.

[59] F. Liu, B. Yi, D. Xing, J. Yu, H. Zhang, J. Memb. Sci. 212 (2003) 213–223, https://doi.org/10.1016/S0376-7388(02)00503-3.

[60] M. Nomnqa, D. Ikhu-Omoregbe, A. Rabiu, Int. J. Chem. Eng. 2016 (2016) 4596251, https://doi.org/10.1155/2016/4596251.

[61] R. Wang, S. Liu, L. Wang, M. Li, C. Gao, Nanomaterials 9 (2019) 9060869, https://doi.org/10.3390/nano9060869.

[62] M. Jung, W. Lee, N.N. Krishnan, S. Kim, G. Gupta, L. Komsiyska, C. Harms, Y. Kwom, D. Henskensmeier, Appl. Surf. Sci. 450(2018) 301-311. 10.1016/j.apsusc.2018.04.198.

[63] C. Sun, A. Zlotorowicz, G. Nawn, E. Negro, F. Bertasi, G. Pagot, K. Vezzu, G. Pace, M. Guarnieri, V. Di Noto, Solid State Ionics 319(2018) 110-116. DOI:10.1016/j.SSI.2018.01.038.

[64] M. Vinothkannan, A. R. Kim, G. Gnana Kumar, D. J. Yoo, RSC Adv. 8(2018), 7494-7508. 10.1039/c7ra12768e.

[65] M. Bernt, A. Siebel, H.A. Gasteiger F314 J. Electrochem. Soc. 165 (2018) F305, https://doi.org/10.1149/2.0641805jes.

[66] Z. Dai, L. Ansaloni, J.J. Ryan, R.J. Spontak, L. Deng, Green Chem. 20 (2018) 1391–1404, https://doi.org/10.1039/c7gc03727a.

[67] K.D.J. Kreuer, Journal of Membrane Science 185 (2001) 29–39, https://doi.org/10.1016/S0376-7388(00)00632-3.

[68] A. K. M. Ali, M. E. A. Ali, A. A. Younes, M. M. Abo El fadl, A. B. Farag, J. Hazard. Mater. 419(2021) 126420. 10.1016/j.jhazmat.2021.126420.

[69] J.D. Kim, A. Donnadio, M.S. Jun, M.L. Di Vona, Int. J. Hydrogen Energy 38 (2013) 1517–1523, https://doi.org/10.1016/j.ijhydene.2012.10.110.

[70] B. H. Goo, A. Z. Al Munsur, O. Choi, Y. Kim, O. J. Kwon, T. H. Kim, ACS Appl. Energy Mater. 3(2020) 11418-11433. 10.1021/acsaem.0c02319.

[71] J.-D. Kim, L.J. Ghil, M.S. Jun, J.K. Choi, H.J. Chang, Y.C. Kim, H.W. Rhee F728 J. Electrochem. Soc. 161 (2014) F724, https://doi.org/10.1149/2.048406jes.

[72] S. Meenakshi, A.K. Sahu, S.D. Bhat, P. Sridhar, S. Pitchumani, A.K. Shukla, Electrochim. Acta 89 (2013) 35–44, https://doi.org/10.1016/j.electacta.2012.11.003.

[73] C. Qin, J. Wang, D. Yang, B. Li, C. Zhang, Catalysts 6 (2016) 6120197, https://doi.org/10.3390/catal6120197.

[74] D. Xing, J. Kerres, Polym. Adv. Technol. (2006) 591–597, https://doi.org/10.1002/pat.758 Improved.

[75] C. Gao, J. Chen, B. Zhang, L. Wang, Polymers (Basel) 12 (2020) 12030652, https://doi.org/10.3390/polym12030652.

[76] R. E. Rosli, A. B. Sulong, W. R. W. Daud, M. A. Zulkefly, T. Husaini, M. I. Rosli, E. H. Majlan, M. A. Haque, Int. J. Hydrogen Energy 42(2017) 9293-9314. 10.1016/j.ijhydene.2016.06.211.

[77] M.S. Jung, T.H. Kim, Y.J. Yoon, C.G. Kang, D.M. Yu, J.Y. Lee, H.J. Kim, Y.T. Hong, J. Memb. Sci. 459 (2014) 72–85, https://doi.org/10.1016/j.memsci.2014.01.072.

[78] S. Darvishmanesh, J. C. Jansen, F. Tasselli, E. Tocci, P. Luis, J. Degrève, E. Drioli, B. V. der Bruggen, J. Memb. Sci. 379(2011) 60-68. 10.1016/j.memsci.2011.05.045.

[79] O.S. Serbanescu, S.I. Voicu, V.K. Thakur, Mater. Today Chem. 17 (2020), https://doi.org/10.1016/j.mtchem.2020.100302.

[80] A. Muthumeenal, A. John Rethinam, A. Nagendran, Solid State Ionics 296 (2016) 296, 106-113. 10.1016/j.ssi.2016.09.010.

[81] Y. Hu, L. Yan, B. Yue, ACS Omega 9 (2020) 13219–13223, https://doi.org/10.1021/acsomega.0c01252.

[82] H.S. Lee, A. Roy, O. Lane, S. Dunn, J.E. McGrath, Polymer 49 (2008) 715–723, https://doi.org/10.1016/j.polymer.2007.12.023.

[83] P. Zhang, W. Li, L. Wang, C. Gong, J. Ding, C. Huang, X. Zhang, S. Zhang, L. Wang, W. Bu, J. Memb. Sci. 596 (2020), https://doi.org/10.1016/j.memsci.2019.117734.

[84] S. Darvishmanesh, F. Tasselli, J. C. Jansen,E. Tocci, F. Bazzarelli, P. Bernardo, P. Luis, J. degrève, E. Driolli, B. V. der Bruggen, J. Memb. Sci. 384(2011) 89-96. 10.1016/j.memsci.2011.09.003.

[85] J. Han, K. Kim, J. Kim, S. Kim, S.W. Choi, H. Lee, J.J. Kim, T.H. Kim, Y.E. Sung, J.C. Lee, J. Memb. Sci. 579 (2019) 70–78, https://doi.org/10.1016/j.memsci.2019.02.048.

[86] N. Jullok, R. V. Hooghten, P. Luis, A. Volodin, C. V. Haesendonck, J. Vermant, B. V. der Bruggen, J. Clean. Prod. 112(2016) 4879-4889. 10.1016/j.jclepro.2015.09.019.

[87] N.A.A. Sani, W.J. Lau, A.F. Ismail, RSC Adv. 5 (2015) 13000–13010, https://doi.org/10.1039/c4ra14284e.

[88] R. Saranya, M. Kumar, R. Tamilarasan, A.F. Ismail, G. Arthanareeswaran, J. Chem. Technol. Biotechnol. 91 (2016) 748–761, https://doi.org/10.1002/jctb.4641.

[89] A. Jomekian, R.M. Behbahani, T. Mohammadi, A. Kargari, Microp. Mesop. Mater. 234 (2016) 43–54, https://doi.org/10.1016/j.micromeso.2016.07.008.

[90] I. Moideen K, A. M. Isloor, A. F. Ismail, A. Obaid, H. K. Fun, Desalin. Water Treat. 57(2016) 19810-19819. 10.1080/19443994.2015.1106985.

[91] A.K. Shukla, J. Alam, M. Alhoshan, L.A. Dass, M.R. Muthumareeswaran, Sci. Rep. 7 (2017) 41976, https://doi.org/10.1038/srep41976.

[92] R. Saranya, G. Arthanareeswaran, A.F. Ismail, N.L. Reddy, M.V. Shankar, J. Kweon, RSC Adv. 7 (2017) 15536–15552, https://doi.org/10.1039/c6ra27314a.

[93] M.C. Nayak, A.M. Isloor, A. Moslehyani, A.F. Ismail, J. Taiwan Inst. Chem. Eng. 77 (2017) 293–301, https://doi.org/10.1016/j.jtice.2017.04.048.

[94] A. K. Shukla, J. Alam, M. Alhoshan, L. A. Dass, F. A. A. Ali, M. R. Muthumareeswaran, U. Mishra, M. A. Ansari, Environ. Sci. Water Res. Technol. 4(2018) 438-448. 10.1039/c7ew00506g.

[95] A. Asadi Tashvigh, L. Luo, T. S. Chung, M. Weber, C. Maletzko, J. Memb. Sci. 545 (2018) 221-228. 10.1016/j.memsci.2017.09.076.

[96] J. Dai, S. Li, J. Liu, J. He, J. Li, L. Wang, J. Lei, J. Memb. Sci. 589 (2019), https://doi.org/10.1016/j.memsci.2019.117261.

[97] T. Arumugham, R.G. Amimodu, N.J. Kaleekkal, D. Rana, J. Env. Sci. 82 (2019) 57–69, https://doi.org/10.1016/j.jes.2019.03.001.

[98] F. Anwar, G. Arthanareeswaran, J. Water Process Eng. 31 (2019), https://doi.org/10.1016/j.jwpe.2019.100844.

[99] A. Naderi, T.S. Chung, M. Weber, C. Maletzko, J. Memb. Sci. 591 (2019), https://doi.org/10.1016/j.memsci.2019.117292.

[100] A. M. Isloor, M. C. Nayak, Inamuddin, B. Prabhu, N. I. Norafiqah, A. M. Asiri, React. Funct. Polym. 139(2019) 170-180. 10.1016/j.reactfunctpolym.2019.02.015.

[101] M. Kumar, S. RaoT, A. M. Isloor, G. P. S. Ibrahim, Inamuddin, N. Ismail, A. F. Ismail, A. M. Asiri, Int. J. Biol. Macromol. 129(2019) 715-727. 10.1016/j.ijbiomac.2019.02.017.

[102] M. Shi, L. Liu, Y. Tong, L. Huang, W. Li, W. Xing, J. App. Poly. Sci. 136 (2019) 47752, https://doi.org/10.1002/app.47752.

[103] G.L. Athens, D. Kim, J.D. Epping, S. Cadars, Y. Ein-Eli, B.F. Chmelka, J. Am. Chem. Soc. 133 (2011) 16023–16036, https://doi.org/10.1021/ja2038529.

[104] M. Chandrashekhar Nayak, A. M. Isloor, Inamuddin, B. Lakshmi, H. M. Marwani, I. Khan, Arab. J. Chem. 13(2019) 4661-4672. 10.1016/j.arabjc.2019.10.007.

[105] W. Kujawski, G. Li, B. Van Der Bruggen, N. Pedišius, J. Šereika, Materials 13 (2020) 13122847, https://doi.org/10.3390/ma13122847.

[106] H.R. Panchami, A.M. Isloor, A.F. Ismail, J. Nanostructure Chem. (Springer 2021.), https://doi.org/10.1007/s40097-021-00416-7.

[107] H. Jang, S.C. Sutradhar, J. Yoo, J. Ha, J. Pyo, C. Lee, T. Ryu, W. Kim, Energies 9 (2016) 9020115, https://doi.org/10.3390/en9020115.

[108] Y. Feng, G. Han, L. Zhang, S.B. Chen, T.S. Chung, M. Weber, C. Staudt, C. Maletzko, Polymer 99 (2016) 72–82, https://doi.org/10.1016/j.polymer.2016.06.064.

[109] H. Shi, Computational Theoretical Chemistry 1112 (2017) 111–122, https://doi.org/10.1016/j.comptc.2017.04.012.

[110] D. Yuan, Y. Qin, S. Li, S. Du, Y. Xu, Q. Weng, P.T. Chen, X. Chen, Z. An, J. Power Sources 484 (2021), https://doi.org/10.1016/j.jpowsour.2020.229265.

[111] G.A. Luduena, T.D. Kuhne, D. Sebastiani, Chem. Mater. 23 (2011) 1424–1429, https://doi.org/10.1021/cm102674u.

[112] K. Yoshimura, L.S. Liebeskind, Macromol. Rapid Commun. 31 (2010) 1725–1730, https://doi.org/10.1002/marc.201000223.

[113] H. Sun, M. Yu, Z. Li, S. Almheiri, Journal of Chemistry 2015 (2015), https://doi.org/10.1155/2015/169680.

[114] S.J. Peighambardoust, S. Rowshanzamir, M. Amjadi, Int. J. Hydrogen Energy 35 (2010) 9349–9384, https://doi.org/10.1016/j.ijhydene.2010.05.017.

[115] A. Rangel-Cárdenas, G. Koper, Materials 10 (2017) 10060576, https://doi.org/10.3390/ma10060576.

[116] Y. Wei, Y. Shang, C. Ni, H. Zhang, X. Li, B. Liu, Y. Men, M. Zhang, W. Hu, Appl. Surf. Sci. 416 (2017) 996–1006, https://doi.org/10.1016/j.apsusc.2017.04.190.

[117] D.J. Kim, H.Y. Hwang, S.Y. Nam, Macromol. Res. 21 (2013) 1194–1200, https://doi.org/10.1007/s13233-013-1162-y.

[118] N.G. Ashar, K.R. Golwalkar, Springer International Publishing Switzerland (2013), https://doi.org/10.1007/978-3-319-02042-6.

[119] Y. Liu, X. Yue, S. Zhang, J. Ren, L. Yang, Q. Wang, G. Wang, Sep. Purif. Technol. 98 (2012) 298–307, https://doi.org/10.1016/j.seppur.2012.06.031.

[120] R.P. Parreño, Y.L. Liu, A.B. Beltran, M.B. Carandang, RSC Adv. 10 (2020) 14198–14207, https://doi.org/10.1039/d0ra01285h.

[121] M. L. Di Vona, E. Sgreccia, M. Tamilvanan, M. Khadhraoui, C. Chassigneux, P. Knauth, J. Memb. Sci. 354(2010) 134–141. 10.1016/j.memsci.2010.02.058.

[122] S. Matsushita, J.D. Kim, Solid State Ionics 316 (2018) 102–109, https://doi.org/10.1016/j.ssi.2017.12.033.

[123] A. Dyck, D. Fritsch, S.P. Nunes, J. Appl. Polym. Sci. 86 (2002) 2820–2827, https://doi.org/10.1002/app.11264.

[124] M. Pirali-Hamedani, S. Mehdipour-Ataei, Des. Monomers Polym. 20 (2017) 54–65, https://doi.org/10.1080/15685551.2016.1231035.

[125] Z. Xiang, X. Zhao, J. Ge, S. Ma, Y. Zhang, H. Na, Chem. Res. Chinese Univ. 32 (2016) 291–295, https://doi.org/10.1007/s40242-016-5344-y.

[126] X. Zhu, J. Huang, C. Jin, S. Zhang, S. Li, B. Jiang, Polym. Bull. 75 (2018) 3739–3751, https://doi.org/10.1007/s00289-017-2232-7.

[127] D. An, B. Wu, G. Zhang, W. Zhang, Y. Wang, J. Power Sources 301 (2016) 204–209, https://doi.org/10.1016/j.jpowsour.2015.09.128.

[128] P. Kulasekaran, B. Maria Mahimai, P. Deivanayagam, RSC Adv. 10(2020) 26521–26527. 10.1039/d0ra04360e.

[129] K. Hunger, N. Schmeling, H.B.T. Jeazet, C. Janiak, C. Staudt, K. Kleinermanns, Membranes 2 (2012) 2040727, https://doi.org/10.3390/membranes2040727.

[130] F. He, S. Wang, D. Yuan, Q. Weng, P. Chen, X. Chen, Z. An, Int. J. Hydrogen Energy 45 (2020) 25262–25275, https://doi.org/10.1016/j.ijhydene.2020.06.149.

[131] D. Yuan, Y. Qin, S. Li, Y. Xu, Q. Weng, P. Chen, X. Chen, Z. An, J. Memb. Sci. 621 (2021), https://doi.org/10.1016/j.memsci.2020.118932.

[132] H.S. Lee, O. Lane, J.E. McGrath, J. Power Sources 195 (2010) 1772–1778, https://doi.org/10.1016/j.jpowsour.2009.10.058.

[133] S.Y. Han, D.M. Yu, Y.H. Mo, S.M. Ah, J.Y. Lee, T.H. Kim, S.J. Yoon, S. Hong, Y.T. Hong, S. So, J. Memb. Sci. 634 (2021), https://doi.org/10.1016/j.memsci.2021.119370.

[134] J.H. Kim, M. Vinothkannan, A.R. Kim, D.J. Yoo, Polymers 12 (2020) 12020325, https://doi.org/10.3390/polym12020325.

[135] G. Titvinidze, K.D. Kreuer, M. Schuster, C.C. De Araujo, J.P. Melchior, W.H. Meyer, Adv. Funct. Mater. 22 (2012) 4456–4470, https://doi.org/10.1002/adfm.201200811.

[136] N. Ureña, M. T. Pérez-Prior, C. del Rio, A. Várez, J. Y. Sanchez, C. Iojoiu, B. Levenfeld, Electrochim. Acta 302(2019) 428-440. 10.1016/j.electacta.2019.01.112.

[137] J. R. Rowlett, Y. Chen, A. T. Shaver, O. Lane, C. Mittelsteadt, H. Xu, M. Zhang, R. B. Moore, S. Mecham, J. E. McGrath, Polymer 54(2013) 6305-6313. 10.1016/j.polymer.2013.09.032.

[138] J. R. Rowlett, V. Lilavivat, A. T. Shaver, Y. Chen, A. Daryaei, H. Xu, C. Mittelsteadt, S. Shimpalee, J. S. Riffle, J. E. McGrath, Polymer 122(2017) 296-302. 10.1016/j.polymer.2017.06.050.

[139] S. Lee, J. Yuk, A.F. Nugraha, Y.G. Shul, S.H. Park, D. Shin, B. Bae, Macromol. Mater. Eng. 303 (2018) 201700650, https://doi.org/10.1002/mame.201700650.

[140] W.H. Lee, K.H. Lee, D.W. Shin, D.S. Hwang, N.R. Kang, D.H. Cho, J.H. Kim, Y.M. Lee, J. Power Sources 282 (2015) 211–222, https://doi.org/10.1016/j.jpowsour.2015.01.191.

[141] B.K. Chen, T.Y. Wu, J.M. Wong, Y.M. Chang, H.F. Lee, W.Y. Huang, A.F. Chen, Polymers 7 (2015) 1046–1065, https://doi.org/10.3390/polym7061046.

[142] J. Shen, X. Lin, J. Liu, X. Li, Macromolecules 52 (2019) 121–134, https://doi.org/10.1021/acs.macromol.8b01389.

[143] X. Jin, L. Li, R. Xu, Q. Liu, L. Ding, Y. Pan, C. Wang, W. Hung, K. Lee, T. Wang, Polymers 10 (2018) 10050539, https://doi.org/10.3390/polym10050539.

[144] H. Hou, M.L. Di Vona, P. Knauth, J. Memb. Sci. 423–424 (2012) 113–127, https://doi.org/10.1016/j.memsci.2012.07.038.

[145] S. Feng, Y. Shang, Y. Wang, G. Liu, X. Xie, W. Dong, J. Xu, V.K. Mathur, J. Memb. Sci. 352 (2010) 14–21, https://doi.org/10.1016/j.memsci.2010.01.040.

[146] P. Zheng, Q. Liu, Z. Li, D. Wang, X. Liu, Polymers 11 (2019) 11060964, https://doi.org/10.3390/polym11060964.

[147] N.N. Krishnan, A. Konovalova, D. Aili, Q. Li, H.S. Park, J.H. Jang, H.J. Kim, D. Henkensmeier, J. Memb. Sci. 588 (2019), https://doi.org/10.1016/j.memsci.2019.117218.

[148] D. Joseph, N.N. Krishnan, D. Henkensmeier, J.H. Jang, S.H. Choi, H.J. Kim, J. Han, S.W. Nam, J. Mater. Chem. A 5 (2017) 409–417, https://doi.org/10.1039/c6ta07653j.

[149] N. N. Krishnan, D. Jospeh, N. M. H. Duong, A. konovalova, J. H. Jang, H. J. Kim, S. W. Nam, D. Henkensmeier, J. Memb. Sci. 544(2017) 416-424. 10.1016/j.memsci.2017.09.049.

[150] J.D. Kim, A. Ohira, H. Nakao, Membranes 10 (2020) 10020031, https://doi.org/10.3390/membranes10020031.

[151] S.D. Mikhailenko, K. Wang, S. Kaliaguine, P. Xing, G.P. Robertson, M.D. Guiver, J. Memb. Sci. 233 (2004) 93–99, https://doi.org/10.1016/j.memsci.2004.01.004.

[152] M.L. Di Vona, E. Sgreccia, S. Licoccia, G. Alberti, L. Tortet, P. Knauth, J. Phys. Chem. B. 113 (2009) 7505–7512, https://doi.org/10.1021/jp9006679.

[153] B. Maranesi, H. Hou, R. Polini, E. Sgreccia, A. Alberti, R. Narducci, P. Knauth, M. L. di Vona, Fuel Cells 13(2013) 107-117. 10.1002/fuce.201200010.

[154] M.L. Di Vona, R. Narducci, L. Pasquini, K. Pelzer, P. Knauth, Int. J. Hydrogen Energy 39 (2014) 14039–14049, https://doi.org/10.1016/j.ijhydene.2014.06.166.

[155] R. Narducci, M.L. Di Vona, A. Marrocchi, G. Baldinelli, Coatings 8 (2018) 8050190, https://doi.org/10.3390/coatings8050190.

[156] D. Wu, L. Wu, J.J. Woo, S.H. Yun, S.J. Seo, T. Xu, S.H. Moon, J. Memb. Sci. 348 (2010) 167–173, https://doi.org/10.1016/j.memsci.2009.10.052.

[157] Y. Zhang, J.D. Kim, K. Miyatake, J. Appl. Polym. Sci. 133 (2016) 44218, https://doi.org/10.1002/app.44218.

[158] P. Bhavani, D. Sangeetha, Int. J. Hydrogen Energy 36 (2011) 14858–14865, https://doi.org/10.1016/j.ijhydene.2011.01.134.

[159] A.K. Sahu, K. Ketpang, S. Shanmugam, O. Kwon, S. Lee, H. Kim, J. Phys. Chem. C 120 (2016) 15855–15866, https://doi.org/10.1021/acs.jpcc.5b11674.

[160] A.K. Mishra, S. Bose, T. Kuila, N.H. Kim, J.H. Lee, Prog. Polym. Sci. 37 (2012) 842–869, https://doi.org/10.1016/j.progpolymsci.2011.11.002.

[161] R. Scipioni, D. Gazzoli, F. Teocoli, O. Palumbo, A. Paolone, N. ibris, S. Brutti, M. A. Navarra, Membranes 4(2014) 123-142. 10.3390/membranes4010123.

[162] V. Di Noto, M. Piga, E. Negro, G.A. Giffin, S. Polizi, T.A. Zawodzinski, RSC Adv. 3 (2013) 18960–18969, https://doi.org/10.1039/C3RA40305J.

[163] R. Deng, W. Han, K.L. Yeung, Catal. Today 331 (2019) 12–17, https://doi.org/10.1016/j.cattod.2018.05.016.

[164] G. Rambabu, S.D. Bhat, F.M.L. Figueiredo, Nanomaterials 9 (2019) 9091292, https://doi.org/10.3390/nano9091292.

[165] M. Notarianni, J. Liu, K. Vernon, N. Motta, Beilstein Journal of Nanotechnol. 7 (2016) 149–196, https://doi.org/10.3762/bjnano.7.17.

[166] R. Vani, S. Ramaprabhu, P. Haridoss, Sustain, Energy Fuels 4 (2020) 1372–1382, https://doi.org/10.1039/c9se01031a.

[167] F. Sun, L.L. Qin, J. Zhou, Y.K. Wang, J.Q. Rong, Y.J. Chen, S. Ayaz, Y.U. Hai-Yin, L. Liu, J. Memb. Sci. 611 (2020), https://doi.org/10.1016/j.memsci.2020.118381.

[168] A.I. Zhbanov, E.G. Pogorelov, Y.C. Chang, ACS Nano 4 (2010) 5937–5945, https://doi.org/10.1021/nn100731u.

[169] Y. L. Liu, Y. H. Su, C. M. Chang, Suryani, D. M. Wang, J. Y. Lai, J. Mater. Chem. 20 (2010) 4409-4416. 10.1039/c000099j.

[170] T. Ko, K. Kim, M.Y. Lim, S.Y. Nam, T.H. Kim, S.K. Kim, J.C. Lee, J. Mater. Chem. A 3 (2015) 20595–20606, https://doi.org/10.1039/c5ta04849d.

[171] K. Kim, J. Bae, M.Y. Lim, P. Heo, S.W. Choi, H.H. Kwon, J.C. Lee, J. Memb. Sci. 525 (2017) 125–134, https://doi.org/10.1016/j.memsci.2016.10.038.

[172] H. Lee, J. Han, K. Kim, J. Kim, E. Kim, H. Shin, J.C. Lee, J. Ind. Eng. Chem. 74 (2019) 223–232, https://doi.org/10.1016/j.jiec.2019.03.012.

[173] J. Han, H. Lee, J. Kim, S. Kim, H. Kim, E. Kim, Y.E. Sung, K. Kim, J.C. Lee, J. Memb. Sci. 612 (2020), https://doi.org/10.1016/j.memsci.2020.118428.

[174] M.Y. Lim, K. Kim, Polymers 10 (2018) 10060569, https://doi.org/10.3390/polym10060569.

[175] J.J. Liu, D. Li, K. Zhang, M. Yang, H. Sun, B. Yang, Small 14 (2018) 201703919, https://doi.org/10.1002/smll.201703919.

[176] W. Jia, B. Tang, P. Wu, Electrochim. Acta 260 (2018) 92–100, https://doi.org/10.1016/j.electacta.2017.11.047.

[177] L. Liu, Y. Lu, Y. Pu, N. Li, Z. Hu, S. Chen, J. Memb. Sci. 640 (2021), https://doi.org/10.1016/j.memsci.2021.119823.

[178] D. Liu, M. Tanaka, H. Kawakami, J. Photopolym. Sci. Technol. 28 (2015) 181–186, https://doi.org/10.2494/photopolymer.28.181.

[179] P.B. Ingabire, X. Pan, A. Haragirimana, N. Li, Z. Hu, S. Chen, React. Funct. Polym. 144 (2019), https://doi.org/10.1016/j.reactfunctpolym.2019.04.006.

[180] P.B. Ingabire, X. Pan, A. Haragirimana, N. Li, Z. Hu, S. Chen, Renew. Energy 152 (2020) 590–600, https://doi.org/10.1016/j.renene.2020.01.072.

[181] P.B. Ingabire, A. Haragirimana, Y. Liu, N. Li, Z. Hu, S. Chen, J. Ind. Eng. Chem. 91 (2020) 213–222, https://doi.org/10.1016/j.jiec.2020.08.002.

[182] Y. Liu, Y. Lu, A. Haragirimana, I.P. Buregeya, N. Li, Z. Hu, S. Chen, Int. J. Hydrogen Energy 45 (2020) 17782–17794, https://doi.org/10.1016/j.ijhydene.2020.04.159.

[183] K. Wang, S. McDermid, J. Li, N. Kremliakova, P. Kozak, C. Song, Y. Tang, J. Zhang, J. Zhang, J. Power Sources 184(2008) 99-103. 10.1016/j.jpowsour.2008.06.008.

[184] K. Oh, O. Kwon, B. Son, D.H. Lee, S. Shanmugam, J. Memb. Sci. 583 (2019) 103–109, https://doi.org/10.1016/j.memsci.2019.04.031.

[185] V. Baglio, F. Lufrano, O. Di Blasi, P. Staiti, V. Antonucci, A.S. Arico, ECS Trans. 41 (2011) 3635730, https://doi.org/10.1149/1.3635730.

[186] V. Ramani, H.R. Kunz, J.M. Fenton, J. Memb. Sci. 266 (2005) 110–114, https://doi.org/10.1016/j.memsci.2005.05.019.

[187] J. Kim, K. Chung, H. Lee, B. Bae, E.B. Cho, Microporous Mesoporous Mater. 236 (2016) 292–300, https://doi.org/10.1016/j.micromeso.2016.01.049.

[188] T. Ko, K. Kim, S.K. Kim, J.C. Lee, Polymer 71 (2015) 70–81, https://doi.org/10.1016/j.polymer.2015.06.055.

[189] G. Kickelbick, Structure and Bonding, Springer International Publishing Switzerland, 2013.

[190] E. Ayandele, B. Sarkar, P. Alexandridis, Nanomaterials 2 (2012) 445–475, https://doi.org/10.3390/nano2040445.

[191] J. Wang, Y. Dai, S. Xu, H. Jiang, R. He, J. Power Sources 506 (2021), https://doi.org/10.1016/j.jpowsour.2021.230217.

[192] F. Chen, W. Dong, F. Lin, W. Ren, X. Ma, Compos. Commun. 24 (2021), https://doi.org/10.1016/j.coco.2021.100676.

[193] M. Janeta, S. Szafert, J. Organomet. Chem. 847 (2017) 173–183, https://doi.org/10.1016/j.jorganchem.2017.05.044.

[194] N. A. Mohamad Nor, J. Jaafar, J.-D. Kim, A. F. Ismail, M. H. D. Othman, M. A Rahman, Arab. J. Sci. Eng. 46(2021) 05088. 10.1007/s13369-020-05088-z.

[195] N. A. Mohamad Nor, J. Jaafar, J. D. Kim, J. Solid State Electrochem. 24(2020) 1185-1195. 10.1007/s10008-020-04594-2.

[196] S.W. Kim, S.Y. Choi, K.-H. Jung, T.-H. Kim, H.W. Rhee, J. Memb. Sci. 566 (2018) 69–76, https://doi.org/10.1016/j.memsci.2018.08.040.

[197] T.N. Thompson, N.Y. Arnett, Polymer 171 (2019) 34–44, https://doi.org/10.1016/j.polymer.2019.03.021.

[198] J. Jaafar, A.F. Ismail, T. Matsuura, K. Nagai, J. Memb. Sci. 382 (2011) 202–2011, https://doi.org/10.1016/j.memsci.2011.08.016.

[199] B. Neethu, G.D. Bhowmick, M.M. Ghangrekar, Biochem. Eng. J. 148 (2019) 170–177, https://doi.org/10.1016/j.bej.2019.05.011.

[200] I. Das, S. Das, R. Dixit, M.M. Ghangrekar, Ionics (Kiel). 26 (2020) 3061–3072, https://doi.org/10.1007/s11581-020-03472-1.

[201] D. Plackett, A. Siu, Q. Li, C. Pan, J.O. Jensen, S.F. Nielsen, A.A. Permyakova, N.J. Bjerrum, J. Memb. Sci. 383 (2011) 78–87, https://doi.org/10.1016/j.memsci.2011.08.038.

[202] M.M. Hasani-Sadrabadi, S.R. Ghaffarian, P. Renaud, RSC Adv. 3 (2013) 19357–19365, https://doi.org/10.1039/c3ra42142b.

[203] C.H. Rhee, H.K. Kim, H. Chang, J.S. Lee, Chem. Mater. 17 (2005) 1691–1697, https://doi.org/10.1021/cm048058q.

[204] E. Paineau, Appl. Sci. 8 (2018) 81011921, https://doi.org/10.3390/app8101921.

[205] K. Kato, K. Inukai, K. Fujikura, T. Kasuga, New J. Chem. 38 (2014) 3591–3599, https://doi.org/10.1039/c4nj00080c.

[206] A.A. Krasilin, E.K. Khrapova, T.P. Maslennikova, Crystals 10 (2020) 10080654, https://doi.org/10.3390/cryst10080654.

[207] I.Y. Jeon, J.B. Baek, Materials 3 (2010) 3654–3674, https://doi.org/10.3390/ma3063654.

[208] K. Li, G. Ye, J. Pan, H. Zhang, M. Pan, J. Memb. Sci. 347 (2010) 26–31, https://doi.org/10.1016/j.memsci.2009.10.002.

[209] X. Li, J. Tao, G. Nie, L. Wang, L. Li, S. Liao, RSC Adv. 4 (2014) 41398–41410, https://doi.org/10.1039/c4ra06519k.

[210] L. Liu, Y. Pu, Y. Lu, N. Li, Z. Hu, S. Chen, J. Memb. Sci. 621 (2021), https://doi.org/10.1016/j.memsci.2020.118972.

[211] M. Dahl, Y. Liu, Y. Yin, Chem. Rev. 14 (2014) 9853–9889, https://doi.org/10.1021/cr400634p.

[212] S.Y. Huang, P. Ganesan, B.N. Popov, Appl. Catal. B Environ. 102 (2011) 171–177, https://doi.org/10.1016/j.apcatb.2010.11.026.

[213] A. Saccà, A. Carbone, I. Gatto, R. Pedicini, A. Freni, A. Patti, E. Passalacqua, Polym. Test. 56 (2016) 10–18, https://doi.org/10.1016/j.polymertesting.2016.09.015.

[214] F.J. Pinar, P. Cañizares, M.A. Rodrigo, D. Ubeda, J. Lobato, RSC Adv. 2 (2012) 1547–1556, https://doi.org/10.1039/c1ra01084k.

[215] Y. Devrim, S. Erkan, N. Baç, I. Eroğlu, Int. J. Hydrogen Energy 34 (2009) 3467–3475, https://doi.org/10.1016/j.ijhydene.2009.02.019.

[216] X. Zhang, Y. Xia, X. Gong, P. Geng, Z. Gao, Y. Wang, J. Appl. Polym. Sci. 137 (2020) 48938, https://doi.org/10.1002/app.48938.

[217] S. Jang, Y.G. Yoon, Y.S. Lee, Y.W. Choi, J. Memb. Sci. 563 (2018) 896–902, https://doi.org/10.1016/j.memsci.2018.06.060.

[218] A.R. Kim, M. Vinothkannan, D.J. Yoo, Compos. Part B, Engineering 130 (2017) 103–118, https://doi.org/10.1016/j.compositesb.2017.07.042.

[219] Y. Liu, P. Huo, J. Ren, G. Wang, High Perform. Polym. 29 (2017) 1037–1048, https://doi.org/10.1177/0954008316667790.

[220] Y. Devrim, Electrochim. Acta 146 (2014) 741–751, https://doi.org/10.1016/j.electacta.2014.08.131.